Because of their different mechanisms of action for improving nitrogen metabolism, BCAA and zinc may further enhance their therapeutic effects when administered concomitantly. Our preliminary data showed more improvement of the ammonia metabolism when these two treatments were combined.[12] In this study, we investigated the effect of combining these supplements using more indices, in addition to serum ammonia levels, and increased the number of patients examined.

METHODS

THIS STUDY ENROLLED 40 cirrhotic patients with the inclusion criteria of diagnosis of cirrhosis based on clinical and laboratory data, serum albumin levels of 3.5 g/dL or less, and serum zinc levels of 70 μg/dL or less. The patients were randomized into two groups to receive either BCAA granules alone or BCAA granules plus zinc sulfate. The BCAA was administered as Livact Granules (Ajinomoto, Tokyo, Japan). One sachet containing 4 g of BCAA, 952 mg L-isoleucine, 1904 mg L-leucine, and 1144 mg L-valine was taken orally after each meal. The zinc sulfate dose was 600 mg/day after each meal for those with blood zinc levels of <50 μg/dL, and 200 mg/day after breakfast for those with blood zinc levels of 50–70 μg/dL.

The patients were followed in the outpatient clinic about every 10 weeks, and the data before the therapy were compared with those of the subsequent visits. During the follow-up period of 5–6 months, changes in blood albumin, Fischer ratio, and ammonia levels were compared between the groups. There were no significant differences between the groups in age, sex, cause of liver disease, liver function test, blood zinc, ammonia, and Fischer ratio at baseline (Table 1).

This clinical investigation was approved by the institutional review board, and oral or written informed consent was obtained from all patients.

Statistical analysis

Continuous variables for patient characteristics of the groups were expressed as mean ± SD and the groups were compared using the Mann–Whitney *U*-test. Non-continuous variables such as sex and cause of liver disease were compared between the groups using the chi-squared test. For therapeutic effects between the groups, the difference between pre- and post-treatment values for each variable (change ratio) was calculated, and the mean ± SD values of the change ratio were compared using the Mann–Whitney *U*-test. Values measured before and after treatment were compared using the Wilcoxon signed rank sum test. The correlations between variables were calculated using Spearman rank correlations. A *P*-value of less than 0.05 was considered statistically significant.

RESULTS

THE BLOOD AMMONIA levels (Fig. 1) increased significantly in the BCAA group ($P = 0.016$), whereas the levels showed a tendency to decrease in the BCAA + zinc group ($P = 0.0707$), with a significant difference in the post/pre treatment change ratio (1.22 ± 0.38 vs. 0.87 ± 0.26, $P = 0.0033$).

The Fischer ratio (Fig. 2) did not show significant difference in the BCAA group ($P = 0.1984$), but increased

Table 1 Characteristics at baseline of cirrhotic patients treated with branched-chain amino acid (BCAA) alone or with BCAA and zinc (BCAA + Zn)

Variable	BCAA ($n = 21$)	BCAA + Zn ($n = 19$)	*P*-value†
Age (years)	65.1 ± 11.3	66.0 ± 9.9	0.745
Sex (male/female)	13/8	10/9	0.553
Etiology (HBV/HBC/other)	3/16/2	1/18/0	0.220
T.Bil (mg/dL)	1.3 ± 0.4	1.2 ± 0.7	0.233
Albumin (g/dL)	3.3 ± 0.2	3.3 ± 0.2	0.525
PT (%)	66.4 ± 12.6	69.1 ± 11.6	0.551
Fischer ratio	1.67 ± 0.48	1.45 ± 0.50	0.093
Ammonia (μg/dL)	46.3 ± 23.0	60.1 ± 36.5	0.194
Zn (μg/dL)	60.2 ± 9.0	58.4 ± 9.2	0.616

†Analysis of continuous variables performed using Mann–Whitney *U*-test; analysis of non-continuous variables performed using chi-squared test. Values are expressed as *n* or as mean ± SD.
HBV, hepatitis B virus carrier; HBC, hepatitis C virus carrier; PT, prothrombin time; T.Bil, total bilirubin.

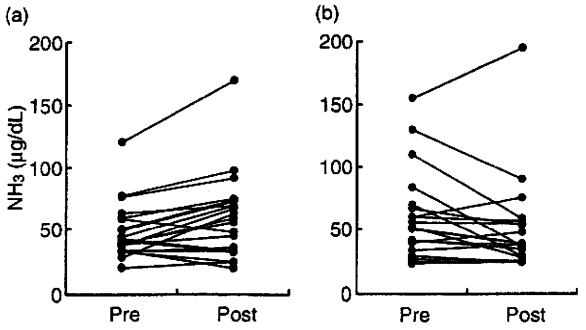

Figure 1 Changes and change ratio in blood ammonia levels after treatment with (a) branched-chain amino acid (BCAA) or (b) BCAA + zinc. Blood ammonia levels increased significantly in the BCAA group ($P = 0.016$), whereas the levels showed a tendency to decrease in the BCAA + zinc group ($P = 0.0707$). There was a significant difference in the post/pre treatment change ratio between the groups (BCAA 1.22 ± 0.38 vs. BCAA + zinc 0.87 ± 0.26, $P = 0.0033$).

significantly in the combined group ($P = 0.0007$). The change ratio also increased more significantly in the combined group (1.08 ± 0.16 vs. 1.22 ± 0.29, $P = 0.0165$).

In contrast, the blood albumin levels (Fig. 3) showed no significant difference between pre- and post-treatment in both groups, and the change ratio also showed no significant difference between the groups (1.03 ± 0.08 vs. 1.01 ± 0.07, $P = 0.4646$).

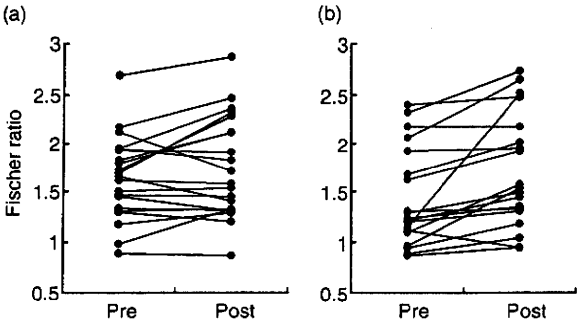

Figure 2 Changes and change ratio in blood Fischer ratio after treatment with (a) branched-chain amino acid (BCAA) or (b) BCAA + zinc. The blood Fischer ratio did not show significant difference in the BCAA group ($P = 0.1984$), but increased significantly in the BCAA + zinc group ($P = 0.0007$). There was a significant difference in the post/pre treatment change ratio between the groups (BCAA 1.08 ± 0.16 vs. BCAA + zinc 1.22 ± 0.29, $P = 0.0165$).

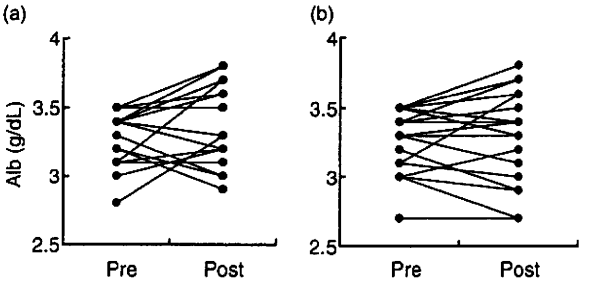

Figure 3 Changes and change ratio in blood albumin levels after treatment with (a) branched-chain amino acid (BCAA) or (b) BCAA + zinc. No significant change was observed before and after treatment both in the BCAA ($P = 0.2227$) and the BCAA + zinc groups ($P = 0.6701$). There was no significant difference in the post/pre treatment change ratio between the groups (BCAA 1.03 ± 0.08 vs. BCAA + zinc 1.01 ± 0.07, $P = 0.4646$).

There was a significant change in the blood zinc levels (Fig. 4) in the BCAA group ($P = 0.0352$), and the levels increased significantly ($P = 0.0005$) in the combined group. The change ratio was also significantly higher in the combined group (1.08 ± 0.15 vs. 1.33 ± 0.27, $P = 0.0018$).

We examined the relationships among ammonia, Fischer ratio, and zinc concentration. Before and after the treatment, there were significant correlations between the Fischer ratio and ammonia (before treatment, $r = -0.646$, $P = 0.0061$; after treatment, $r = -0.529$, $P = 0.0248$). However, there was no significant correlation between zinc and ammonia (before treatment, $r = 0.001$, $P = 0.9970$; after treatment,

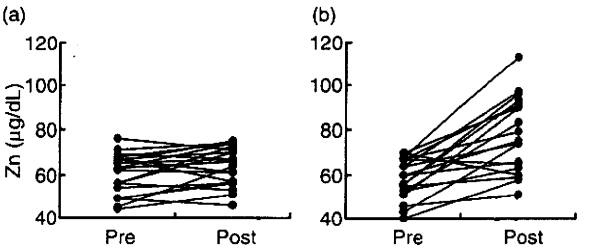

Figure 4 Changes and change ratio in blood zinc levels after treatment with (a) branched-chain amino acid (BCAA) or (b) BCAA + zinc. The blood zinc levels increased significantly in the BCAA group ($P = 0.0352$) and in the BCAA + zinc group ($P = 0.0005$). There was a significant difference in the post/pre treatment change ratio between the groups (BCAA 1.08 ± 0.15 vs. BCAA + zinc 1.33 ± 0.27, $P = 0.0018$).

$r = -0.124$, $P = 0.5985$), and was no significant correlation between zinc and the Fischer ratio (before treatment, $r = 0.121$, $P = 0.6062$; after treatment, $r = 0.346$, $P = 0.1421$). In this study, the albumin concentration before the treatment did not correlate with the change ratio of the Fischer ratio, albumin or ammonia in either group (data not shown).

DISCUSSION

SUPPLEMENTATION OF BCAA has been indicated to improve prognosis and reduce the incidence of complications.[6–8] This study demonstrated that combination treatment with BCAA and zinc supplements in cirrhotic liver patients with hypoalbuminemia or hypozincemia showed significantly higher efficacy in correcting amino acid imbalance and significantly greater ability to metabolize ammonia than when BCAA was given alone during the 6 months of the study period. Because zinc deficiency is a common disorder in patients with liver cirrhosis,[10–14] the addition of zinc supplementation to conventional therapy can be important for treatment of liver cirrhosis.

The amino acid imbalance (i.e. decreased BCAA levels) in liver cirrhosis may be partly caused by the fact that a decreased ability to process ammonia in the liver increases the proportion of unprocessed ammonia, and BCAA is consumed when the unprocessed ammonia is processed via glutamine synthesis in the skeletal muscle.[9] Supplementation of BCAA alone in this disease state does not eliminate the cause, namely decreased ability to process ammonia in the liver, although it contributes to the correction of amino acid imbalance. Therefore, its efficacy is limited in terms of ammonia metabolism. In fact, Horst *et al.*[6] reported that when proteins mainly composed of BCAA are administered to patients with liver cirrhosis, the blood ammonia levels increase to the same degree as when normal protein is administered.

The correction of zinc deficiency in liver cirrhosis leads to further improvement of the ability of the liver to metabolize nitrogen (mainly ammonia).[11–14] In addition, in the present study, the blood ammonia levels significantly increased in the BCAA group but showed a tendency to decrease in the combined group, with a significant difference in the change ratio between the groups. This is inferred to be due to an increased ability to metabolize ammonia in the liver with zinc administration as compared to the nitrogen load from BCAA supplementation. The accelerated processing of ammonia via glutamine synthetase in the skeletal muscle cannot, of course, be excluded.[15] Also in the study of Marchesini *et al.*,[14] zinc supplementation greatly improved the nitrogen metabolism in the liver, and the ammonia levels decreased more due to an increase in metabolic function than to metabolism in the skeletal muscle. Further investigation is necessary to reach a definite conclusion.

In this study, the Fischer ratio improved more significantly in the combined group. In view of the fact that in liver cirrhosis, BCAA is consumed mainly during ammonia metabolism in the skeletal muscle,[9,12] the improvement of ammonia detoxification in the liver by zinc administration in the combined group may have consequently decreased the amount of ammonia that had to be processed in the skeletal muscle, resulting in a decrease of BCAA consumption. In this case, the administered BCAA that was not consumed in the skeletal muscle was likely to have contributed to an improvement of the blood amino acid balance. The mechanism remains to be elucidated in future work.

Despite the alleviation of the amino acid imbalance in the combined group, the blood albumin levels were similar between the two groups in this study. BCAA, particularly leucine, has been shown to act as a signal for stimulating protein synthesis via m-TOR,[16] and improvement of the Fischer ratio probably influences protein synthesis, or albumin synthesis. The relatively short period of the present investigation may have prevented recognition of a difference in the ability to synthesize albumin. To more accurately examine the clinical efficacy with respect to prognosis and the incidence of other complications, a longer-term study is needed.

In this study, before and after the treatment, there were significant correlations between the Fischer ratio and ammonia. However, there was no significant correlation between zinc and ammonia, and between zinc and the Fischer ratio. In our previous study,[17] we found a significant correlation between zinc and ammonia, and between zinc and the Fischer ratio. These differences may have arisen from a difference in the range of liver diseases examined. In the present study, we enrolled patients with liver cirrhosis only, while in our previous study, subjects consisted of those with chronic hepatitis and liver cirrhosis.

In conclusion, more improvement in disorders of nitrogen metabolism in patients with liver cirrhosis was observed when BCAA was administered together with zinc than when given alone. Further investigation is necessary to determine the detailed mechanisms of the action and longer-term clinical efficacy.

REFERENCES

1 Christensen E, Schlichting P, Fauerholdt L *et al.* Prognostic value of Child-Turcotte criteria in medically treated cirrhosis. *Hepatology* 1984; 4: 430–5.
2 Alberino F, Gatta A, Amodio P *et al.* Nutrition and survival in patients with liver cirrhosis. *Nutrition* 2001; 17: 445–50.
3 Tajika M, Kato M, Mohri H *et al.* Prognostic value of energy metabolism in patients with liver cirrhosis. *Nutrition* 2002; 18: 229–34.
4 Moriwaki H, Miwa Y, Tajika M *et al.* Branched-chain amino acids as a protein- and energy-source in liver cirrhosis. *Biochem Biophys Res Comm* 2004; 313: 405–9.
5 Fischer JE, Baldessarini RI. False neurotransmitter and hepatic failure. *Lancet* 1971; 2: 75–80.
6 Horst D, Grace ND, Conn HO *et al.* Comparison of dietary protein with an oral branched chain-enriched amino acid treatment in chronic hepatic encephalopathy: a randomized controlled trial. *Hepatology* 1984; 4: 279–87.
7 Marchesini G, Bianchi G, Merli M *et al.* Nutritional supplementation with branched-chain amino acids in advanced cirrhosis: a double blind, randomized trial. *Gastroenterology* 2003; 124: 1792–801.
8 Muto Y, Sato S, Watanabe A *et al.* Effects of oral branched-chain amino acid granules on event-free survival in patients with liver cirrhosis. *Clin Gastroenterol Hepatol* 2005; 3: 705–13.
9 Hayashi M, Ohnishi H, Kawade Y, Muto Y, Takahashi Y. Augmented utilization of branched-chain amino acids by skeletal muscle in decompensated liver cirrhosis in special relation to ammonia detoxication. *Gastroenterol Jpn* 1981; 16: 64–70.
10 Bode JC, Hanisch P, Henning H, Koenig W, Richter FW, Bode C. Hepatic zinc content in patients with various stages of alcoholic liver disease and in patients with chronic active and chronic persistent hepatitis. *Hepatology* 1988; 8: 1605–9.
11 Reding P, Duchateau J, Bataille C. Oral zinc supplementation improves hepatic encephalopathy. Results of a randomized controlled trial. *Lancet* 1984; ii: 493–5.
12 Katayama K. Ammonia and hepatic encephalopathy. *Hepatol Res* 2004; 30S: S71–8.
13 Riggio O, Merli M, Capocaccia L *et al.* Zinc supplementation reduces blood ammonia and increases liver ornithine transcarbamylase activity in experimental cirrhosis. *Hepatology* 1992; 16: 785–9.
14 Marchesini G, Fabbri A, Bianchi G, Brizi M, Zoli M. Zinc supplementation and amino acid-nitrogen metabolism in patients with advanced cirrhosis. *Hepatology* 1996; 23: 1084–92.
15 Lockwood AH, McDonald JM, Reiman RE *et al.* The dynamics of ammonia metabolism in man. Effects of liver disease and hyperammoninemia. *J Clin Invest* 1979; 63: 449–60.
16 Hara K, Yonezawa K, Weng QR *et al.* Amino acid sufficiency and mTOR regulate p70S6 kinase and eIF-4E BP1 through a common effector mechanism. *J Biol Chem* 1998; 273: 14484–94.
17 Katayama K, Ooka Y, Kikkawa S *et al.* The relationship between amino acid-nitrogen metabolism and plasma zinc in patients with chronic liver disease. *Kanzou* 2001; 42: 120–5.

Research Article

EASL EUROPEAN ASSOCIATION FOR THE STUDY OF THE LIVER | JOURNAL OF HEPATOLOGY

Possible involvement and the mechanisms of excess *trans*-fatty acid consumption in severe NAFLD in mice

Noriyuki Obara[1], Koji Fukushima[1], Yoshiyuki Ueno[1,*], Yuta Wakui[1], Osamu Kimura[1], Keiichi Tamai[1], Eiji Kakazu[1], Jun Inoue[1], Yasuteru Kondo[1], Norihiko Ogawa[2], Kenta Sato[3], Tsuyoshi Tsuduki[3], Kazuyuki Ishida[4], Tooru Shimosegawa[1]

[1]*Division of Gastroenterology, Tohoku University Graduate School of Medicine, 1-1 Seiryo, Aobaku, Sendai 980-8574, Japan;* [2]*Division of Advanced Surgical Science and Technology, Graduate School of Medicine, Tohoku University, Sendai, Japan;* [3]*Laboratory of Food and Biomolecular Science, Graduate School of Agricultural Science, Tohoku University, Sendai, Japan;* [4]*Department of Pathology, Tohoku University Hospital, Sendai, Japan*

Background & Aims: Excessive *trans*-fatty acids (TFA) consumption has been thought to be a risk factor mainly for coronary artery diseases while less attention has been paid to liver disease. We aimed to clarify the impact of TFA-rich oil consumption on the hepatic pathophysiology compared to natural oil.

Methods: Mice were fed either a low-fat (LF) or high-fat (HF) diet made of either natural oil as control (LF-C or HF-C) or partially hydrogenated oil, TFA-rich oil (LF-T or HF-T) for 24 weeks. We evaluated the liver and body weight, serological features, liver lipid content and composition, liver histology and hepatic lipid metabolism-related gene expression profile. In addition, primary cultures of mice Kupffer cells (KCs) were evaluated for cytokine secretion and phagocytotic ability after incubation in *cis*- or *trans*-fatty acid-containing medium.

Results: The HF-T-fed mice showed significant increases of the liver and body weights, plasma alanine-aminotransferase, free fatty acid and hepatic triglyceride content compared to the HF-C group, whereas the LF-T group did not differ from the LF-C group. HF-T-fed mice developed severe steatosis, along with increased lipogenic gene expression and hepatic TFA accumulation. KCs showed increased tumor necrosis factor secretion and attenuated phagocytotic ability in the TFA-containing medium compared to its *cis*-isomer.

Conclusions: Excessive consumption of the TFA-rich oil up-regulated the lipogenic gene expression along with marked hepatic lipid accumulation. TFA might be pathogenic through causing severe steatosis and modulating the function of KCs. The quantity and composition of dietary lipids could be responsible for the pathogenesis of non-alcoholic steatohepatitis.

Keywords: *trans*-Fatty acid; NASH; NAFLD; Metabolic syndrome; Kupffer cell.
Received 16 September 2009; received in revised form 18 January 2010; accepted 26 February 2010; available online 22 April 2010
*Corresponding author. Tel.: +81 22 717 7171; fax: +81 22 717 7177.
E-mail address: yueno@mail.tains.tohoku.ac.jp (Y. Ueno).

Abbreviations: NAFLD, non-alcoholic fatty liver disease; NASH, non-alcoholic steatohepatitis; FFA, free fatty acid; LPS, lipopolysaccharide; TFA, *trans*-fatty acid; ALT, alanine-aminotransferase; LF(-C or -T), low-fat (control or TFA-rich) diet; HF(-C or -T), high-fat (control or TFA-rich) diet; KCs, Kupffer cells (KCs); AST, aspartate-aminotransferase; TG, triglyceride; ELISA, Enzyme-Linked ImmunoSorbent Assay; HDL, high density lipoprotein; (V)LDL, (very) low density lipoprotein; NAS, NAFLD activity score; TBARS, thiobarbituric acid reactive substances; TNFα, tumor necrosis factor α; IL-6, interleukin-6; SD, standard deviation; iNOS, inducible nitric oxide synthase; TGF-β, transforming growth factor-β; SREBP-1, sterol regulatory element-binding protein-1; FAS, fatty acid synthase; ACC, acetyl CoA carboxylase; PPAR, peroxisome proliferator activated receptor; PGC-1β, PPARγ coactivator-1β; PUFA, polyunsaturated fatty acid; MUFA, monounsaturated fatty acid; SFA, saturated fatty acid.

Introduction

In concordance with the prevalence of obesity, the incidence of non-alcoholic fatty liver disease (NAFLD) has increased and is nowadays recognized as the most common liver disease [2]. It is known that a part of NAFLD can progress to non-alcoholic steatohepatitis (NASH), liver fibrosis, cirrhosis and hepatocellular carcinoma [9]. Nevertheless, the mechanisms of NAFLD-to-NASH transition remain to be clarified; NAFLD appears to originate from the dysregulation of hepatic lipid metabolism as a part of the metabolic syndrome accompanied by visceral obesity, dyslipidemia, atherosclerosis, and insulin resistance [25]. According to the hypothetical theory named the 2-hit theory [5], the secondary hit to NAFLD that can be due to free fatty acid (FFA)s, oxidative stress, lipopolysaccharide (LPS) and inflammatory cytokines, causes NASH as a consequence.

In terms of the "first hit", the lipid accumulation in the liver is induced by high-fat diets [6,23] that include various lipid species. Such dietary lipid species uniquely affect the obesity phenotype, liver histology and gene expression pattern in the rat liver [3]. In this context, lipid species could play a potential role in the pathogenesis of NAFLD and/or NASH.

trans-Fatty acid (TFA) is produced through the industrial hardening of the vegetable oils to make the products more stable and robust, and thus easier to handle or store. Excess consumption of TFA is known as a risk factor for coronary artery diseases, insulin resistance and obesity accompanied by systemic inflammation, the features of metabolic syndrome [20,29]. Nevertheless, little is known about the effects on the liver induced by lipids.

Fast-foods, containing large amount of TFA in the form of margarine, spreads or frying oils, cause body-weight gain and abnormal serum alanine-aminotransferase (ALT) elevations in healthy subjects [15]. In addition, TFA-rich chow leads to hepatic steatosis [30], ALT elevations and insulin resistance in mice [17]; although the mechanisms have not been completely clarified. Therefore, we aimed to investigate the impact of the dietary lipid species and their quantities on the pathogenicity of hepatic inflammation and steatosis in mice comparing in particular natural oil and industrially produced partially hydrogenated TFA-rich oil of the same origin.

Materials and methods

Animal treatment

All the animal experiments were conducted under the approval of the Institutional Animal Care and Use Committees of Tohoku University. Female C57BL/6Njcl mice (8–10 weeks) were randomly assigned to four groups ($n = 6$ per group) and fed the designated chows (ORIENTAL YEAST Co. Ltd., Tokyo, Japan) *ad libitum* for 24 weeks, respectively. Low-fat diet (LF) and high-fat diet (HF) were made of either natural canola oil as control oil (LF-C and HF-C) or industry produced partially hydrogenated canola oil as TFA-rich oil (28.5% TFA/total fat, LF-T and HF-T), respectively (Table 1). After 12 h of fasting, the mice were sacrificed under diethylether anesthesia and the livers were removed and weighed. The divided livers were either stored at −80 °C for lipid, protein and gene expression analysis, or fixed in 4% paraformaldehyde and embedded in paraffin for histological evaluation. Standard chow-fed female C57BL/6Njcl mice (6–10 weeks) were used as a source of primary Kupffer cells (KCs).

Chemistry

Plasma aspartate-aminotransferase (AST), ALT, triglyceride (TG) and total cholesterol were measured with FUJI DRI-CHEM 7000 (FUJIFILM, Tokyo, Japan) at Biomedical Research Core of Tohoku University Graduate School of Medicine. Plasma adiponectin (AdipoGen, Seoul, Korea) and leptin (RayBio, GA, USA) were measured by Enzyme-Linked ImmunoSorbent Assay (ELISA). Plasma FFA, high density lipoprotein (HDL)-cholesterol and (very) low density lipoprotein ((V)LDL)-cholesterol were measured by enzymatic assay kits (BioVision, CA, USA).

Histology and immunohistochemistry

The thin-sliced specimens were stained with hematoxylin and eosin to evaluate steatosis and inflammation or Sirius red to evaluate fibrosis of the liver. The histology was scored by the NAFLD activity score (NAS) [16]. KCs were stained with anti-F4/80 monoclonal antibody (Abcam, Cambridge, UK) and neutrophils were detected by myeroperoxidase immunostaining (Abcam). Apoptosis was evaluated by TUNEL method using an ApopTag kit (Chemicon, CA, USA).

Table 1. Diet compositions.

	Low-fat diet		High-fat diet	
	Control oil (LF-C) kcal%	TEA-rich oil (LF-T) kcal%	Control (HF-C) kcal%	TEA-rich (HF-T) kcal%
Diet compositions				
Protein	13.8	13.8	18.8	18.8
Carbohydrate	74.4	74.4	17.6	17.6
Over all fat	11.8	11.8	63.6	63.6
Fat composition (g/100 g)				
Saturated	7.8	21.7	7.8	21.7
(*cis*-)Monounsaturated	62.5	45.3	62.5	45.3
Polyunsaturated	29.7	4.5	29.7	4.5
trans- (%)		28.5		28.5

Immunoblot analysis and real-time RT-PCR

Liver protein extracts were evaluated by immunoblot analysis with the following primary antibodies: phosphor-AKT (Thr308 and Ser473), total AKT (Cell Signaling Technology, Danvers, MA) and β-actin (Sigma, MO, USA). RNA extracted from the livers was subjected to real-time RT-PCR analysis using the specifically designed primer sets purchased form TAKARA BIO Perfect Real Time Support System (TAKARA BIO INC., Tokyo, Japan) and One Step SYBR Prime Script RT-PCR Kit II (TAKARA BIO INC.), and only PGC-1β was analyzed using the specifically designed TaqMan primer set and 1-step kit (Applied Biosystems, CA, USA). All results were normalized by GAPDH as the internal control.

Lipidomic analysis of the liver

Hepatic TG and FFA content were measured by enzymatic assay kit (BioVision) and were normalized by the liver weight. Hepatic lipid peroxide was evaluated by measuring TBARS (thiobarbituric acid reactive substances, Cayman Chemical Company, USA) in the liver and was normalized by the protein level [18]. Total lipids from the liver were extracted by Folch's procedure [10]. The lipids were methylated and evaluated by gas chromatography as previously reported [31].

Isolation and culture of primary Kupffer cells

KCs were isolated as reported previously [28]. Briefly, the mice livers were digested by two-step collagenase perfusion. The minced livers were subjected to the gradient centrifugation of Percoll (Sigma) and succeeding counterflow centrifugal elutriation. The viabilities of the obtained cells evaluated by trypan blue staining were more than 85%, and the purity was more than 90% determined by the population of CD11b positive cells counted by FACS Calibur (Becton Dickinson, Tokyo, Japan). KCs were suspended in RPMI1640 medium with 10% fetal bovine serum and antibiotics (100 U/ml penicillin G, 100 μg/ml streptomycin sulfate) and incubated overnight at 37 °C in 5% CO_2 incubator for the succeeding examinations.

Fatty acid treatment

Fatty acids (Larodan Fine Chemicals, Malmo, Sweden) were dissolved in RPMI1640 medium with 1% fatty acid-free bovine serum albumin (Calbiochem, Darmstadt, Germany) and adjusted to a final concentration of 200 μM with 1% bovine serum albumin, 1% ITS-A supplement (GIBCO, CA, USA) and antibiotics same as above. After overnight incubation, KCs were washed and the medium was changed to fatty acid-containing medium or fatty acid-free medium as the control, and incubated for another 24 h.

Cytokine production by KCs stimulated with lipopolysaccharide

After 24 h incubation, KCs were stimulated by LPS (100 ng/ml, SIGMA) combined with LPS-binding protein (200 pg/ml, ALEXIS BIOCHEMICALS, Lausanne, Switzerland) for 6 h, and the cell viability was determined by MTS assay (3-(4,5-dimethylthiazol-2-yl)-5-(3-carboxymethoxyphenyl)-2-(4-sulfophenyl)-2*H*-tetrazolium, inner salt and phenazine ethosulfate, Promega, Tokyo, Japan). The supernatants were subjected to ELISA (Thermo Fisher Scientific Inc., IL, USA) for the evaluation of the tumor necrosis factor-alfa (TNFα) and interleukin-6 (IL-6) production.

Phagocytotic ability of KCs

After 24 h incubation, KCs were incubated at 37 °C for 1 h with 1 μm latex beads (75 ng/ml, SIGMA) or at 4 °C in the fatty acid-free medium as control. After incubation, the cells were washed 3 times, detached with trypsin/EDTA and analyzed by FACS calibur [1].

Statistical analysis

The results are shown as the mean ± standard deviation (SD), and were analyzed by SPSS software (SPSS INC., Tokyo, Japan).

The differences between the groups were tested by ANOVA, followed by Tukey post hoc test. A p values less than 0.05 were considered statistically significant.

Results

Physiological and biochemical characteristics

Body weight was similar between LF-fed mice, increased in HF-fed mice compared to LF-fed mice, and strikingly HF-T-fed mice weighed 1.3-fold more than HF-C-fed mice (Table 2). Liver weight was significantly increased in only HF-T-fed mice by approximately 2-fold compared to the other groups. The liver–body weight ratio was significantly increased by 1.2- and 1.6-fold in LF-T-fed and HF-T-fed mice, respectively, compared to the corresponding control groups with the same dietary composition, and decreased by approximately 20% in the HF-C-fed mice compared to the LF-C-fed mice.

Plasma AST, ALT, TG, FFA and leptin were similar between the LF groups irrespective of the dietary lipid source, but in the LF-T group, total cholesterol, HDL-cholesterol, (V)LDL-cholesterol and adiponectin were significantly decreased compared to the LF-C group (Table 2). In contrast, some serum markers were elevated in the HF-T group compared to the HF-C group, particularly AST, ALT, TG, total cholesterol, (V)LDL-cholesterol, FFA and leptin were significantly increased. As for the control oil-fed mice, total cholesterol, HDL-cholesterol, (V)LDL-cholesterol and adiponectin were lower, whereas plasma leptin was higher in HF-C-fed than in LF-C-fed mice. Between TFA-rich oil-fed mice, all serum markers except adiponectin were also significantly higher in HF-T-fed than in LF-T-fed mice.

Liver histology

There were few lipid droplets in LF-C-fed mice liver. Mild microvesicular and macrovesicular steatosis was present around zone 1 in LF-T-fed mice livers and abundant large lipid droplets around zones 1 and 2 in HF-C-fed mice livers. Inflammation and ballooning degeneration were minimal in these groups (Fig. 1A). However, the HF-T-fed mice livers were characterized by foamy, prominent microvesicular steatosis throughout the lobe and some macrovesicular lipid droplets in zones 1 and 2. Most of the hepatocytes were expanded with marked small lipid droplets that surrounded the nuclei, and the severely expanded hepatocytes presented the phenotype of ballooning degeneration (Fig. 1A); moreover, some of the fatty hepatocytes were surrounded by infiltrated neutrophils confirmed by immunostaining for myeloperoxidase, forming lipogranuloma (Fig. 1B) accompanied by ballooning hepatocytes (Fig. 1C). The number of neutrophils was increased in HF-T-fed mice livers (Fig. 1D). However, when evaluated by NAS, the HF-T group did not show significant differences (Table 2).

To investigate the involvement of KCs in the pathological difference between the HF-C group and HF-T group, we performed immunohistochemical staining for F4/80, a macrophage-restricted surface glycoprotein. F4/80-positive cells were more prevalent in the HF-T group (Fig. 1E). Although fibrosis was not identified visually by Sirius red staining in any of the groups (not shown), collagen type1, α1 mRNA expression in the liver, as an early fibrosis marker, increased only in HF-T-fed mice by 3.6-fold compared to LF-C-fed mice (Fig. 1F). TUNEL assay did not reveal conspicuous apoptotic hepatocytes in each group, however some non-parenchymal cells were TUNEL positive (Supplementary Fig. 1).

Lipid and lipid peroxide content and fatty acid composition of liver

The hepatic total lipid (Fig. 2A), TG (Fig. 2B), FFA (Fig. 2C) and lipid peroxide contents (Fig. 2D) did not differ between the LF-C and LF-T groups. On the other hand, reflecting the marked liver weight gain and histological steatotic changes, hepatic total lipid, TG and lipid peroxide content were significantly increased in the HF-T group compared to the HF-C group, while FFA content did not differ. All of these markers had a tendency to be elevated in the HF groups compared to the LF groups and when compared between the corresponding dietary oil-fed groups, although the TG increase in HF-C-fed mice was not statistically significant.

Table 2. Influence of *trans*-fatty acid-rich oil intake for the physiological and biochemical characteristics.

	Low-fat diet		High-fat diet	
	Control oil (LF-C)	TFA-rich oil (LF-T)	Control oil (HF-C)	TFA-rich oil (HF-T)
Body weight (g)	24.4 ± 2.1	23.1 ± 1.3	31.8 ± 3.6[‡]	40.9 ± 7.0[*‡†]
Liver weight (g)	1.08 ± 0.16	1.22 ± 0.08	1.11 ± 0.11	2.40 ± 1.01[*‡†]
Liver–body weight ratio (%)	4.5 ± 0.4	5.4 ± 0.2[*]	3.5 ± 0.3[‡]	5.6 ± 1.6[*†]
Plasma characteristics				
Aspartate-aminotransferase (IU/L)	95.2 ± 12.4	82.5 ± 20.8	136.8 ± 47.0	262.2 ± 72.0[*‡†]
Alanine-aminotransferase (IU/L)	48.8 ± 15.0	37.0 ± 7.3	50.4 ± 10.9	244.0 ± 105.7[*‡†]
Triglyceride (mg/dl)	60.3 ± 19.2	51.0 ± 12.8	62.4 ± 14.8	124.8 ± 45.0[*‡†]
Total cholesterol (mg/dl)	77.0 ± 8.9	47.5 ± 6.1[*]	55.2 ± 5.0	87.8 ± 10.1[*‡]
HDL-cholesterol (mg/dl)	51.6 ± 8.3	26.2 ± 3.9[*]	33.3 ± 7.2[‡]	38.6 ± 5.0[‡†]
(V)LDL-cholesterol (mg/dl)	16.8 ± 2.1	12.0 ± 1.5[*]	11.9 ± 1.0[‡]	17.4 ± 1.7[*‡]
Free fatty acids (nmol/ml)	1.77 ± 0.38	1.43 ± 0.31	1.99 ± 0.58	3.64 ± 0.42[*‡†]
Adiponectin (μg/ml)	25.5 ± 1.4	18.2 ± 1.4[*]	20.0 ± 1.5[‡]	20.0 ± 1.4[†]
Leptin (ng/L)	5.6 ± 0.7	5.3 ± 0.6	13.8 ± 2.0[‡]	23.7 ± 2.3[*‡†]
Total: HDL-cholesterol ratio	1.54 ± 0.06	2.33 ± 0.5[*]	1.71 ± 0.37	2.25 ± 0.87[†]
NAFLD activity score				
Steatosis	0.33 ± 0.52	0.17 ± 0.41	1.67 ± 0.82[‡]	1.17 ± 0.41[‡]
Inflammation	0.33 ± 0.52	0.33 ± 0.52	0.83 ± 0.75	1.00 ± 0.63
Ballooning	0.00 ± 0.00	1.00 ± 0.63[*]	1.00 ± 0.00[‡]	1.67 ± 0.82[†]

All values are means ± SD (n = 6 per each group).
[*] Significantly different from the corresponding control group with the same dietary composition; p <0.05.
[‡] Significantly different from the low-fat diet with the same dietary lipid as a source; p <0.05.
[†] Significantly different from low-fat control diet group; p <0.05.

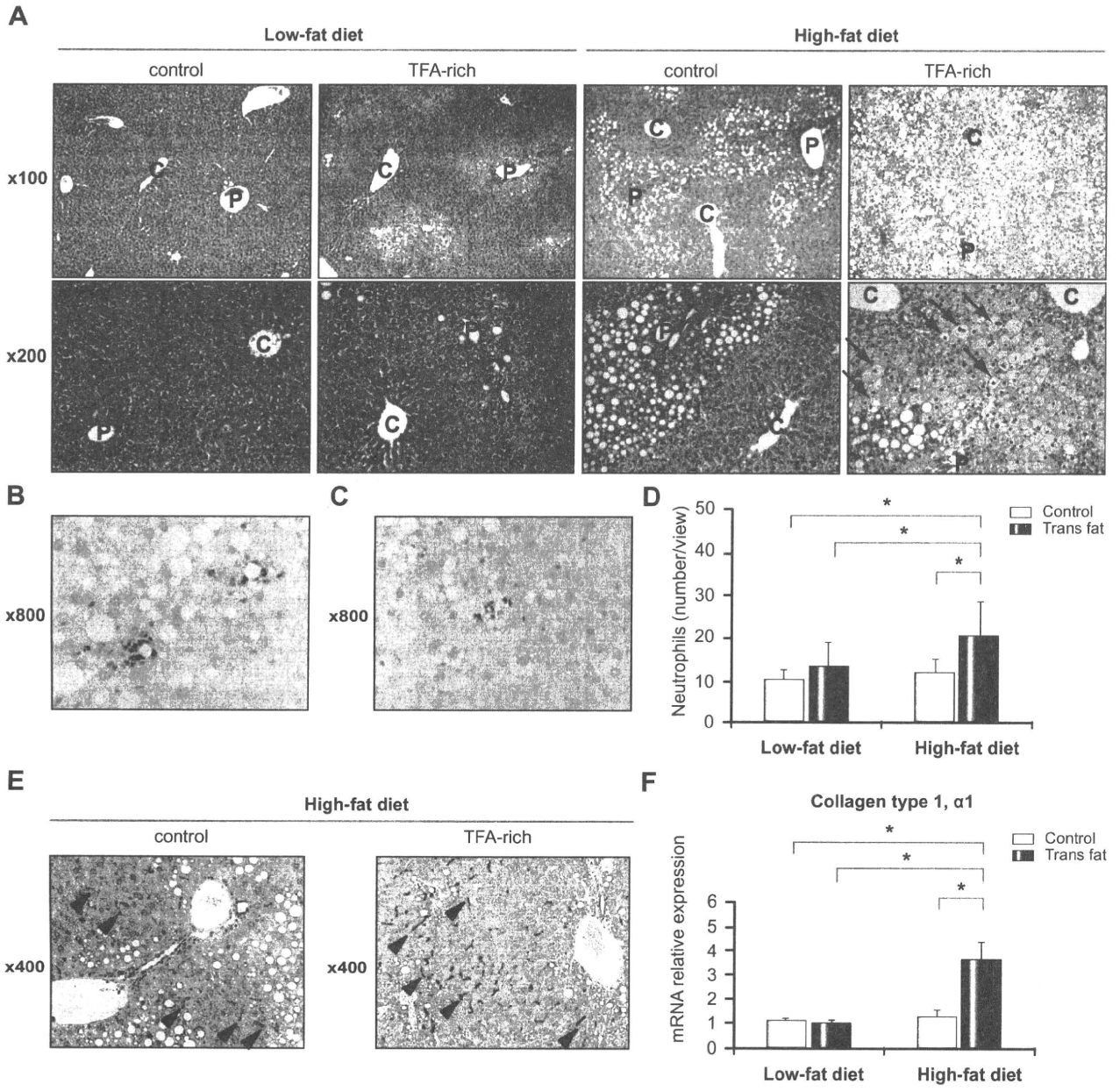

Fig. 1. Distinct steatotic features of the liver. (A) Representative liver histology stained with H&E. Remarkably expanded hepatocytes with extensive small lipid droplets make a feature of ballooning degeneration (arrows). Neutrophils confirmed by myeloperoxidase staining were (B) forming lipogranulomas and (C) surrounding the ballooning degenerated hepatocytes. (D) The number of neutrophils is increased in HF-T-fed mice liver. (E) KCs were detected by anti-F4/80 immunohistochemical staining (arrow heads). (F) Quantitative RT-PCR revealed elevation of collagen type 1, α1 mRNA expression in liver of HF-T-fed mice. P, portal tract; C, central vein. *p <0.05.

We evaluated the lipid composition of the liver to examine the pathological condition in the model. Compared to the LF-C group, the sum of total polyunsaturated fatty acid (PUFA), n-6 PUFA and n-3 PUFA was decreased in the LF-T group, but did not differ significantly in the other groups (Fig. 2E.). In the HF-C group, the sum of saturated fatty acid (SFA) and monounsaturated fatty acid (MUFA) was decreased, and total PUFA, n-6 PUFA and n-3 PUFA were increased compared to the LF-C group. However, in the HF-T group, total PUFA and n-6 PUFA decreased significantly compared to the LF-C group, and their proportions were similar to those of the LF-T group. The potentially beneficial lipid n-3 PUFA that is thought to prevent insulin resistance and hepatic steatosis [11], was increased even in the HF-T group compared to the LF-T group, the level of which was similar to that of the LF-C group.

The content of individual fatty acids in the liver coordinated nearly synergistically with the sum of the content of the fatty acids in the same unsaturation grade (Fig. 2E and Table 3). The unique accumulation of elaidic acid (18:1(9-*trans*)), chief component of dietary TFA, was noteworthy in the LF-T and HF-T groups. The content of arachidonic acid (20:4n-6) alone decreased to 70% only in the HF-T group, which was similar to the LF-T group in

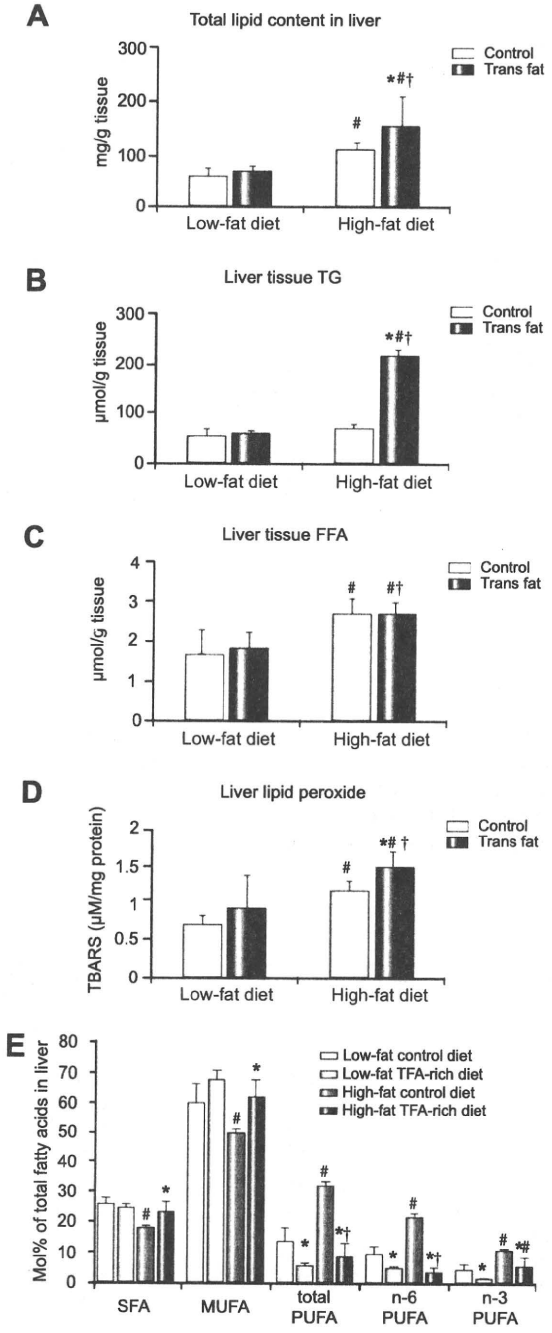

Fig. 2. Lipid accumulation in the liver. (A) Total lipid, (B) TG, and (C) FFA in the liver were measured and normalized to the tissue weight. (D) Lipid peroxide in the liver was measured and normalized by each amount of protein. (E) The hepatic fatty acid composition analyzed by gas chromatography was organized as follows: SFA, saturated fatty acid; MUFA, *cis*-monounsaturated fatty acid; PUFA, polyunsaturated fatty acid; *n*-6, *n*-6 PUFA; and *n*-3, *n*-3 PUFA ($n = 6$ for each group). *Significantly different from the control group with the same dietary composition; #significantly different from the low-fat diet with same dietary oil; †significantly different from LF-C-fed and HF-T-fed group.

terms of linoleic acid (18:2*n*-6), the precursor of arachidonic acid. Except for elaidic acid and arachidonic acid, there were no specific alterations for the HF-T group.

Cytokine-, adipokine- and lipid metabolism-related gene expression in liver

Real-time RCR showed that TNFα and inducible nitric oxide synthase (iNOS) mRNA expression increased in the HF groups compared to the LF groups by approximately 2-fold when evaluated for each C or T group (Table 4), while no difference was seen in IL-6 and transforming growth factor-β (TGF-β) mRNA expression in liver among all groups. In addition, adiponectin receptor 1 and 2 gene expression was measured as adipokine related genes, but they did not differ among all groups.

To examine the potential mechanisms of hepatic steatosis by the TFA-rich diet, we determined the expression of known mediators of lipogenesis, fatty acid oxidation and TG excretion in liver, the imbalance of which is thought to lead to steatosis. Sterol regulatory element-binding protein-1 (SREBP-1) induces fatty acid synthase (FAS) and acetyl CoA carboxylase (ACC), and is implicated in steatosis [27]. In relation to hepatic fatty acid synthesis, the mRNA expression of SREBP-1 was significantly elevated in the LF-T, HF-C and HF-T groups when compared to the LF-C group, whereas FAS and ACC were elevated significantly only in the HF-T group (Table 4). Peroxisome proliferator activated receptor γ (PPARγ) is also implicated in steatosis [33]. The expression of PPARγ1 did not differ among the groups, while PPARγ2 was significantly elevated 13-fold in the HF-C group and, remarkably, 50-fold in the HF-T group. Although, the expression of PPARγ coactivator-1β (PGC-1β), known to coactivate the SREBP-1 and stimulate lipogenic gene expression [19], was decreased in HF-fed mouse livers. The fatty acid oxidation-related genes of PPARα and carnitine palmitoyl transferase-1, and the TG excretion-related genes of microsomal triglyceride transfer protein and apolipoprotein B did not differ among the groups; fatty acid oxidation-related genes showed a tendency to be decreased in the LF-T group, but without statistical significance.

Concerning cholesterol metabolism-related gene expression in liver, SREBP-2 was increased in the HF groups, but was not affected by the dietary lipid sources. Hydroxymethylglutaryl-CoA synthase-1 and reductase were significantly increased and apolipoprotein A-1, a component of HDL, was decreased only in the HF-T group, while they did not change in the LF-T group, which showed an alteration of plasma cholesterol fraction (Table 4).

Phosphorylation status of AKT in high-fat diet-fed mice livers

As Koppe et al. suggested that TFA feeding increased insulin resistance in mice [17], and to determine if the exacerbating effects of TFA intake on liver were associated with increased insulin resistance, we evaluated the hepatic phosphorylation status of AKT (Fig. 3A). The phospho-AKT(Thr308) level was significantly decreased (Fig. 3B) and the phospho-AKT(Ser473) level was also decreased, but without statistical significance (Fig. 3C) as determined by densitometrical analysis.

TFA increases TNFα production and alters phagocytotic ability of KCs

The *cis*- or *trans*-fatty acid-containing medium showed no cytotoxicity towards KCs when compared to the fatty acid-free control medium (Fig. 4A). TNFα production of KCs induced by LPS was increased in both the C18:1 and C18:2 TFA-containing medium compared to that of *cis*-structural isomer-containing

Table 3. Individual fatty acid composition of the liver.

		Low-fat diet		High-fat diet	
		Control oil (LF-C)	TFA-rich oil (LF-T)	Control oil (HF-C)	TFA-rich oil (HF-T)
SFA					
Myristic	14:0	0.6 ± 0.1	0.5 ± 0.0	0.3 ± 0.1‡	0.4 ± 0.1*†
Palmitic	16:0	21.0 ± 1.6	19.2 ± 1.1	12.1 ± 0.6‡	18.7 ± 3.6*
Stearic	18:0	3.7 ± 0.8	3.6 ± 0.6	4.6 ± 0.6	3.3 ± 1.2
Arachidic	20:0	0.6 ± 0.3	1.0 ± 0.1*	0.6 ± 0.3	0.9 ± 0.3
MUFA					
Palmitoleic	16:1 *n*-7	6.9 ± 4.9	7.9 ± 4.8	2.5 ± 0.2	4.9 ± 1.0
Oleic	18:1	53.4 ± 6.7	59.8 ± 2.3	47.4 ± 1.3	57.2 ± 4.8*‡†
Elaidic	18:1 (9-*trans*)	0.0 ± 0.0	2.2 ± 0.5*	0.3 ± 0.2	6.2 ± 2.4*‡†
PUFA					
Linoleic	18:2 *n*-6	6.5 ± 2.1	2.1 ± 0.4*	18.1 ± 1.6‡	2.6 ± 1.4*†
α-Linolenic	18:3 *n*-3	0.6 ± 0.4	0.0 ± 0.0*	3.2 ± 0.5‡	0.2 ± 0.2‡
Dihomo-γ-linolenic	20:3 *n*-6	0.2 ± 0.1	0.2 ± 0.1	0.5 ± 0.2‡	0.2 ± 0.2
Arachidonic	20:4 *n*-6	2.5 ± 0.9	2.2 ± 0.5	2.6 ± 0.6	0.6 ± 0.3*‡†
Eicosapentaenoic	20:5 *n*-3	0.4 ± 0.2	0.1 ± 0.0	1.4 ± 0.1‡	1.2 ± 0.9‡†
Docosapentaenoic	22:5 *n*-3	0.2 ± 0.1	0.0 ± 0.0	0.8 ± 0.0‡	0.4 ± 0.3*‡†
Docosahexaenoic	22:6 *n*-3	3.0 ± 1.1	1.0 ± 0.3	5.2 ± 0.4	3.2 ± 2.4

The relative percentage (mean ± SD) of each fatty acid to the total fatty acids is presented (n = 6 per each group).
* Significantly different from the corresponding control group with the same dietary composition; p <0.05.
‡ Significantly different from the low-fat diet with the same dietary lipid as a source; p <0.05.
† Significantly different from low-fat control diet group; p <0.05.

medium (Fig. 4B). However, IL-6 production by KCs did not differ between *cis*- and *trans*-fatty acid-containing medium for both C18:1 and C18:2, respectively (Fig. 4C). The phagocytotic ability of KCs incubated in *trans*-C18:1-containing medium was lower than that in *cis*-C18:1-containing medium (Fig. 4D), while the influence of the structural difference of C18:2 fatty acid was small (Fig. 4E).

Discussion

Both of the dietary lipid species [3] and their amounts [6,23] are known to affect hepatic steatosis and inflammation. TFAs have been mainly linked with coronary heart disease, possibly by decreasing HDL-cholesterol and increasing LDL-cholesterol [20,29]; while little attention has been paid to liver disease, even

Table 4. Cytokine-, adipokine- and lipid metabolism-related gene expression in liver.

		Low-fat TFA-rich (LF-T)	High-fat control (HF-C)	High-fat TFA-rich (HF-T)
Cytokine and adipokine				
Tumor necrosis factor	TNF	0.98 ± 0.20	2.11 ± 0.73‡	1.94 ± 0.77‡†
Interleukin-6	IL-6	1.30 ± 0.28	1.16 ± 0.14	1.10 ± 0.25
Transforming growth factor-β	TGB-β	0.86 ± 0.17	1.35 ± 0.50	0.98 ± 0.22
Nitric oxide synthase 2, inducible	iNOS	1.29 ± 0.34	2.23 ± 0.75‡	2.69 ± 0.74‡†
Adiponectin receptor 1	AdipoR1	1.01 ± 0.17	1.29 ± 0.29	1.21 ± 0.25
Adiponectin receptor 2	AdipoR2	0.92 ± 0.16	1.20 ± 0.22	1.28 ± 0.26
Lipogenesis				
Fatty acid synthase	FAS	1.36 ± 0.21	0.79 ± 0.12	1.69 ± 0.46*†
Acetyl-CoA carboxylase	ACC	1.27 ± 0.10	0.80 ± 0.05	1.49 ± 0.37*†
Sterol regulatory element-binding protein-1	SREBP-1	3.76 ± 0.51*	1.93 ± 0.23‡	4.69 ± 0.17*‡†
Peroxisome proliferator activated receptor γ1	PPARγ1	1.45 ± 0.42	1.58 ± 0.48	1.29 ± 0.26
Peroxisome proliferator activated receptor γ2	PPARγ2	1.88 ± 0.33	12.92 ± 6.04‡	50.18 ± 3.61*‡†
PPARγ coactivator-1β	PGC-1β	0.81 ± 0.10	0.61 ± 0.15‡	0.59 ± 0.12‡†
Fatty acid oxidation				
Peroxisome proliferator activated receptor α	PPARα	0.51 ± 0.23	1.25 ± 0.48	1.28 ± 0.41
Carnitine palmitoyl transferase-1	CPT-1	0.63 ± 0.11	1.03 ± 0.34	1.08 ± 0.57
Triglyceride excretion				
Microsomal triglyceride transfer protein	MTP	1.04 ± 0.16	0.92 ± 0.11	0.91 ± 0.11
Apolipoprotein B	ApoB	1.11 ± 0.15	1.20 ± 0.13	1.15 ± 0.09
Cholesterol metabolism				
Sterol regulatory element-binding protein-2	SREBP-2	0.87 ± 0.15	1.66 ± 0.25	1.69 ± 0.34
Hydroxymethylglutaryl-CoA synthase-1	HMGCs1	1.03 ± 0.11	1.60 ± 0.26	4.56 ± 0.73*‡†
Hydroxymethylglutaryl-CoA reductase	HMGCr	0.99 ± 0.13	1.22 ± 0.32	2.93 ± 0.44*‡†
Apolipoprotein A-1	ApoA1	0.93 ± 0.09	1.26 ± 0.21	0.61 ± 0.11*‡†

All results are expressed as the relative fold change compared to the low-fat control diet group ± SD (n = 6 per each group).
* Significantly different from the corresponding control group with the same dietary composition; p <0.05.
‡ Significantly different from the low-fat diet with the same dietary lipid as a source; p <0.05.
† Significantly different from low-fat control diet group; p <0.05.

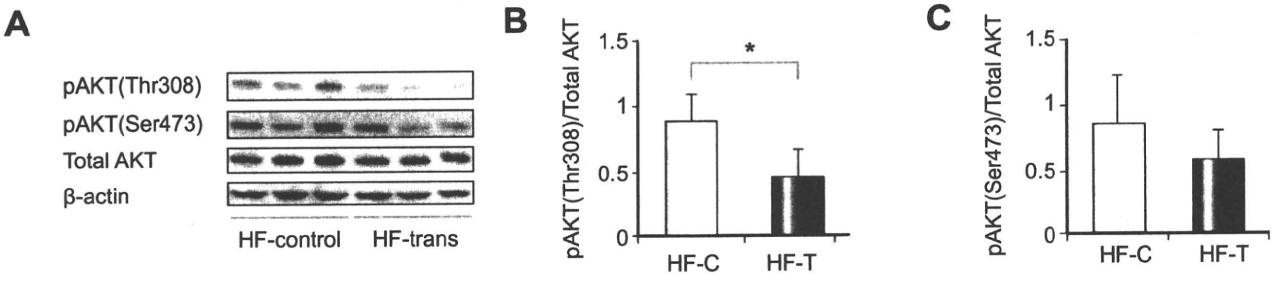

Fig. 3. Effect of excessive TFA consumption of AKT in the high-fat diet-fed mice liver. (A) Representative pictures of phospho-AKT (Thr308 and Ser473), total AKT and β-actin Western blots as well as densitometric analysis of the (B) pAKT(Thr308) or (C) pAKT(Thr473)/total AKT ratio. *p <0.05.

though a few studies have reported that hepatic steatosis [30] and ALT elevation [17] were induced by a TFA-rich diet in mice, the mechanisms remain to be clarified. In agreement with this, the HF-T group showed severe steatosis with a significant transaminase elevation, while HF-C-fed mice only showed moderate steatosis without liver injury, in addition we showed that relatively small amounts of TFA-rich oil intake do not induce severe steatosis and liver injury in the current study. Interestingly, the plasma cholesterol fraction was significantly altered even in the LF-T group in association with the elevation of the total: HDL-cholesterol ratio, a risk factor index of coronary artery disease [22]. The alteration of the plasma cholesterol fraction might be partially explained by changes in the cholesterol metabolism-related gene expressions in the HF-T group, but not in the LF-T group. We could not determine why the cholesterol fraction was altered in the LF-T group, but it might be partially due to the modified membrane fluidity induced by TFA intake [14]. That a relatively small TFA intake could affect the cholesterol fraction but not the liver might be the reason why less attention has been paid to the liver until recently.

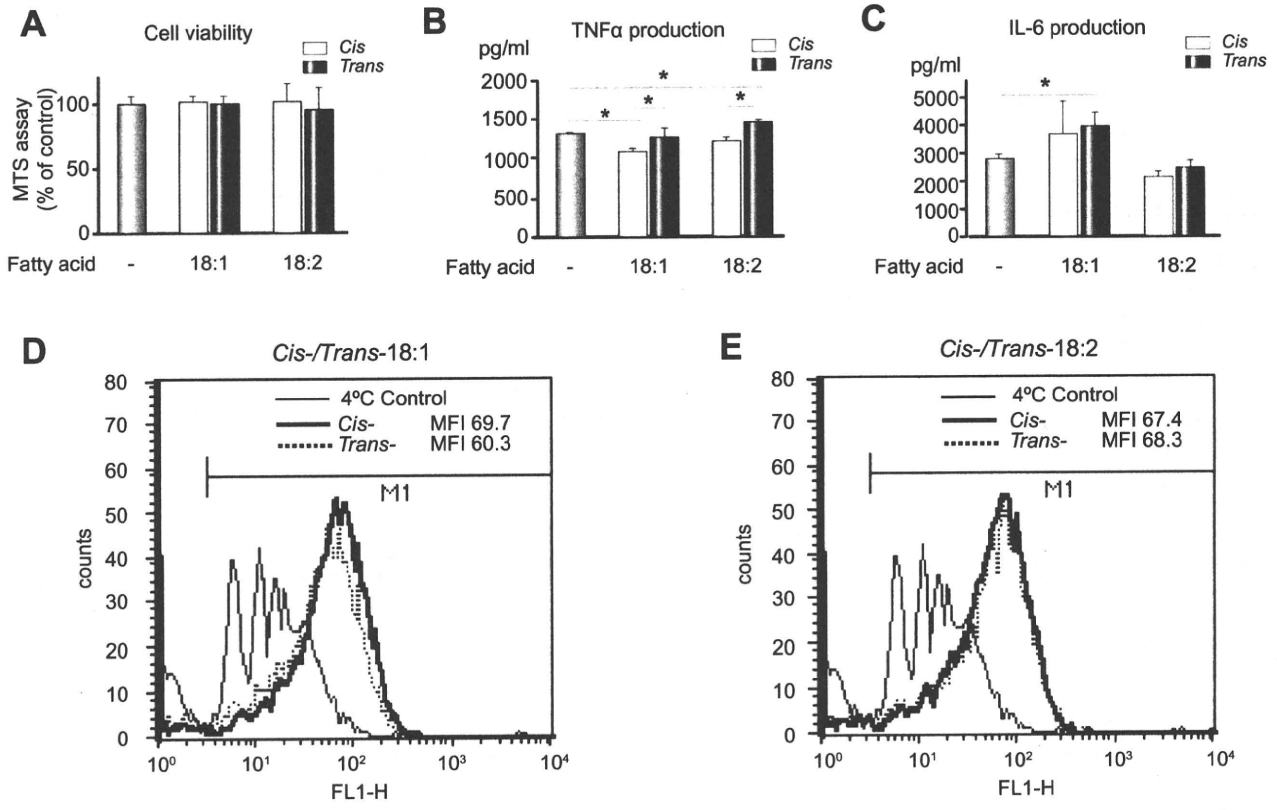

Fig. 4. The impact of *cis-/trans*-fatty acid on the cytokine production and phagocytotic ability of KCs. (A) No fatty acids (200 μM) shows cytotoxicity for primary KCs after 24 h incubation, but (B) increases TNFα production in both C18:1 and C18:2-TFA-containing medium compared to its *cis*-structural isomer. (D) IL-6 production increases in C18:1-containing medium and remains unchanged in C18:2-containing medium, whereas the *cis*- or *trans*-structural difference does affect the results. The influence of the C18:1 (D) and C18:2 (E) *cis-/trans*-fatty acid on the phagocytotic ability of KCs is measured by flow cytometry analysis. MFI: mean fluorescence intensity (n = 8 for each group, A–C). *p <0.05.

One of the noted biochemical changes seen in the HF-T group was the elevation of plasma FFA, almost all of which is derived from adipose tissue and accumulates in the liver as TG in a dose-dependent fashion [7]. The increase of plasma FFA might be due to the TFA incorporation in the adipocyte plasma membrane resulting in decreased membrane fluidity, accompanied by increased adipose tissue insulin resistance as evidenced by increased lipolysis, decreased antilipolysis and decreased glucose uptake in rat adipocytes [14]. In addition, in contrast to TG, the circulating FFAs [21] and accumulation of FFAs in liver [32] are known to exert lipotoxicity to hepatocytes, so the significant increase of the plasma FFA in the HF-T group might affect the pathophysiology. On the other hand, hepatic FFA was higher in HF than LF irrespective of the dietary lipid sources, and it was reported that forced high-fat feeding induced NASH in mice, while usual high-fat intake does not [6]. Hepatic FFA accumulation remained unaltered among healthy, NAFLD and NASH subjects liver [24], so it might not be necessary for the progression to NASH but could be a exacerbating factor in the case of excess fat consumption. Therefore, elevated plasma FFA and accumulated hepatic lipid peroxide [23] would contribute synergistically to the liver injury in this model.

A previous study reported that TFA intake decreased the arachidonic acid level and induced insulin resistance in adipose tissue, probably due to the decreased membrane fluidity [14], and the present study also revealed a decrease of the arachidonic acid level in the liver and lower phosphorylation status of AKT which could reflect the hepatic insulin resistant status in the HF-T group. In addition, a human lipidomic analysis of NAFLD/NASH liver described a decrease of arachidonic acid and unaltered levels of precursor linoleic acid, but the study did not address TFA consumption [24]. Although, the mechanisms of the arachidonic acid decrease and involvement in the insulin resistance and progression to NASH remain to be clarified, these common findings might suggest that TFA intake influences both the liver and adipose tissue in a somewhat similar fashion in NASH patients and people who consume excess TFAs.

Typical pathological findings in human NAFLD/NASH patients such as macrovesicular lipid deposit and inflammation are usually identified around zone 3, though the mice liver showed lipid deposits around zone 1 even in the control lipid-fed group. Microvesicular lipid droplets were remarkable in the HF-T group, so it might be difficult to assess the pathological changes using a human scoring system such as NAS. The pathological differences might be due to a specific problem, since the pediatric NAFLD is known to show histological findings around zone 1 [26], which might be related to the dietary habit of consuming excess TFAs from snacks and first food.

Although the expression of proinflammatory cytokines such as TNFα [30] and IL-1β [17] have been shown to be induced in the mice liver by TFA-rich diets, this was not the case in the current study. However, a previous study reported that, among hypercholesterolemic subjects, the production of TNFα by cultured mononuclear cells was increased by a TFA-rich soy bean margarine diet compared with a natural soybean oil diet [12], and we showed KCs increased TNFα production in TFA-containing medium compared to that of *cis*-structural isomer-containing medium. Accordingly, pathophysiological conditions induced by TFA consumption could be partially due to alterations in the monocyte/macrophage ability in proinflammatory cytokine production and phagocytosis, and KCs in particular may play important roles in the local circumstances.

With regard to the adipokines, the adiponectin levels were not changed between the HF-C and HF-T group, but plasma leptin was significantly increased in the HF-T group. Leptin is an appetite-suppressing and body weight-regulating adipokine, and is even related to liver regeneration and fibrosis [13]; hyperleptinemia might be related directly to the elevation of type1 collagen α1 mRNA expression in the liver.

In terms of the severe steatosis of the model, the lipogenetic genes such as FAS, ACC, SREBP-1 and PPARγ2 were coordinately induced, but PGC-1β was not. PGC-1β is known to be induced in the liver by short term high-fat feeding, to coactivate SREBP-1, but to reduce hepatic fat accumulation. However, since it was not investigated in this study, the decrease of PGC-1β gene expression might be due to long term feeding or any other factors, such as the relatively low carbohydrate diet. It was reported that a TFA-rich diet suppressed the PPARγ gene expression in rat adipose tissue [8], and that lipogenic gene expressions in the liver and the adipose tissue are reciprocal modulations [4], which might reflect the core mechanisms of the heterotopic fat accumulation *in vivo*.

In summary, excess TFA consumption induces significant hepatic steatosis accompanied by augmentation of the hepatic lipogenic gene expressions, FFA influx into the liver, and the hepatic accumulation of lipid peroxide. The hepatic accumulation of TFA and the reduction of the arachidonic acid content were the lipidomic properties in this model. Together with their potential induction of local cytokines by KCs, lipid species including TFA may play a pivotal role in the development of non-alcoholic fatty liver diseases.

Acknowledgements

This study was supported in part from Health and Labour Sciences Research Grants for the Research on Measures for Intractable Diseases (from the Ministry of Health, Labour and Welfare of Japan), from Grant-in-Aid for Scientific Research C (20590755 to KF) from Japanese Society of Promotion of Science (JSPS).

Conflicts of interest

The authors who have taken part in this study declared that they do not have anything to disclose regarding funding or conflict of interest with respect to this manuscript.

Supplementary data

Supplementary data associated with this article can be found, in the online version, at doi:10.1016/j.jhep.2010.02.029.

References

[1] Babior BM. Oxygen-dependent microbial killing by phagocytes (first of two parts). N Engl J Med 1978;298:659–668.
[2] Browning JD, Szczepaniak LS, Dobbins R, Nuremberg P, Horton JD, Cohen JC, et al. Prevalence of hepatic steatosis in an urban population in the United States: impact of ethnicity. Hepatology 2004;40:1387–1395.
[3] Buettner R, Parhofer KG, Woenckhaus M, Wrede CE, Kunz-Schughart LA, Scholmerich J, et al. Defining high-fat-diet rat models: metabolic and molecular effects of different fat types. J Mol Endocrinol 2006;36:485–501.
[4] Cao H, Gerhold K, Mayers JR, Wiest MM, Watkins SM, Hotamisligil GS. Identification of a lipokine, a lipid hormone linking adipose tissue to systemic metabolism. Cell 2008;134:933–944.

[5] Day CP, James OF. Steatohepatitis: a tale of two "hits"? Gastroenterology 1998;114:842–845.
[6] Deng QG, She H, Cheng JH, French SW, Koop DR, Xiong S, et al. Steatohepatitis induced by intragastric overfeeding in mice. Hepatology 2005;42:905–914.
[7] Donnelly KL, Smith CI, Schwarzenberg SJ, Jessurun J, Boldt MD, Parks EJ. Sources of fatty acids stored in liver and secreted via lipoproteins in patients with nonalcoholic fatty liver disease. J Clin Invest 2005;115:1343–1351.
[8] Duque-Guimaraes DE, de Castro J, Martinez-Botas J, Sardinha FL, Ramos MP, Herrera E, et al. Early and prolonged intake of partially hydrogenated fat alters the expression of genes in rat adipose tissue. Nutrition 2009;25: 782–789.
[9] Farrell GC, Larter CZ. Nonalcoholic fatty liver disease: from steatosis to cirrhosis. Hepatology 2006;43:S99–S112.
[10] Folch J, Lees M, Sloane Stanley GH. A simple method for the isolation and purification of total lipides from animal tissues. J Biol Chem 1957;226: 497–509.
[11] Gonzalez-Periz A, Horrillo R, Ferre N, Gronert K, Dong B, Moran-Salvador E, et al. Obesity-induced insulin resistance and hepatic steatosis are alleviated by omega-3 fatty acids: a role for resolvins and protectins. FASEB J 2009;23:1946–1957.
[12] Han SN, Leka LS, Lichtenstein AH, Ausman LM, Schaefer EJ, Meydani SN. Effect of hydrogenated and saturated, relative to polyunsaturated, fat on immune and inflammatory responses of adults with moderate hypercholesterolemia. J Lipid Res 2002;43:445–452.
[13] Honda H, Ikejima K, Hirose M, Yoshikawa M, Lang T, Enomoto N, et al. Leptin is required for fibrogenic responses induced by thioacetamide in the murine liver. Hepatology 2002;36:12–21.
[14] Ibrahim A, Natrajan S, Ghafoorunissa R. Dietary trans-fatty acids alter adipocyte plasma membrane fatty acid composition and insulin sensitivity in rats. Metabolism 2005;54:240–246.
[15] Kechagias S, Ernersson A, Dahlqvist O, Lundberg P, Lindstrom T, Nystrom FH. Fast-food-based hyper-alimentation can induce rapid and profound elevation of serum alanine aminotransferase in healthy subjects. Gut 2008;57:649–654.
[16] Kleiner DE, Brunt EM, Van Natta M, Behling C, Contos MJ, Cummings OW, et al. Design and validation of a histological scoring system for nonalcoholic fatty liver disease. Hepatology 2005;41:1313–1321.
[17] Koppe SW, Elias M, Moseley RH, Green RM. Trans fat feeding results in higher serum alanine aminotransferase and increased insulin resistance compared with a standard murine high-fat diet. Am J Physiol Gastrointest Liver Physiol 2009;297:G378–G384.
[18] Larter CZ, Yeh MM, Haigh WG, Williams J, Brown S, Bell-Anderson KS, et al. Hepatic free fatty acids accumulate in experimental steatohepatitis: role of adaptive pathways. J Hepatol 2008;48:638–647.
[19] Lin J, Yang R, Tarr PT, Wu PH, Handschin C, Li S, et al. Hyperlipidemic effects of dietary saturated fats mediated through PGC-1beta coactivation of SREBP. Cell 2005;120:261–273.
[20] Lopez-Garcia E, Schulze MB, Meigs JB, Manson JE, Rifai N, Stampfer MJ, et al. Consumption of trans fatty acids is related to plasma biomarkers of inflammation and endothelial dysfunction. J Nutr 2005;135:562–566.
[21] Malhi H, Gores GJ. Molecular mechanisms of lipotoxicity in nonalcoholic fatty liver disease. Semin Liver Dis 2008;28:360–369.
[22] Mensink RP, Zock PL, Kester AD, Katan MB. Effects of dietary fatty acids and carbohydrates on the ratio of serum total to HDL cholesterol and on serum lipids and apolipoproteins: a meta-analysis of 60 controlled trials. Am J Clin Nutr 2003;77:1146–1155.
[23] Milagro FI, Campion J, Martinez JA. Weight gain induced by high-fat feeding involves increased liver oxidative stress. Obesity (Silver Spring) 2006;14: 1118–1123.
[24] Puri P, Baillie RA, Wiest MM, Mirshahi F, Choudhury J, Cheung O, et al. A lipidomic analysis of nonalcoholic fatty liver disease. Hepatology 2007;46:1081–1090.
[25] Reid AE. Nonalcoholic steatohepatitis. Gastroenterology 2001;121:710–723.
[26] Schwimmer JB, Behling C, Newbury R, Deutsch R, Nievergelt C, Schork NJ, et al. Histopathology of pediatric nonalcoholic fatty liver disease. Hepatology 2005;42:641–649.
[27] Shimano H, Horton JD, Hammer RE, Shimomura I, Brown MS, Goldstein JL. Overproduction of cholesterol and fatty acids causes massive liver enlargement in transgenic mice expressing truncated SREBP-1a. J Clin Invest 1996;98:1575–1584.
[28] Su GL, Klein RD, Aminlari A, Zhang HY, Steinstraesser L, Alarcon WH, et al. Kupffer cell activation by lipopolysaccharide in rats: role for lipopolysaccharide binding protein and toll-like receptor 4. Hepatology 2000;31: 932–936.
[29] Sun Q, Ma J, Campos H, Hankinson SE, Manson JE, Stampfer MJ, et al. A prospective study of trans fatty acids in erythrocytes and risk of coronary heart disease. Circulation 2007;115:1858–1865.
[30] Tetri LH, Basaranoglu M, Brunt EM, Yerian LM, Neuschwander-Tetri BA. Severe NAFLD with hepatic necroinflammatory changes in mice fed trans fats and a high-fructose corn syrup equivalent. Am J Physiol Gastrointest Liver Physiol 2008;295:G987–G995.
[31] Tsuzuki T, Tokuyama Y, Igarashi M, Nakagawa K, Ohsaki Y, Komai M, et al. Alpha-eleostearic acid (9Z11E13E-18:3) is quickly converted to conjugated linoleic acid (9Z11E-18:2) in rats. J Nutr 2004;134:2634–2639.
[32] Yamaguchi K, Yang L, McCall S, Huang J, Yu XX, Pandey SK, et al. Inhibiting triglyceride synthesis improves hepatic steatosis but exacerbates liver damage and fibrosis in obese mice with nonalcoholic steatohepatitis. Hepatology 2007;45:1366–1374.
[33] Zhang YL, Hernandez-Ono A, Siri P, Weisberg S, Conlon D, Graham MJ, et al. Aberrant hepatic expression of PPARgamma2 stimulates hepatic lipogenesis in a mouse model of obesity, insulin resistance, dyslipidemia, and hepatic steatosis. J Biol Chem 2006;281:37603–37615.

Hepatitis B Virus Replication Could Enhance Regulatory T Cell Activity by Producing Soluble Heat Shock Protein 60 From Hepatocytes

Yasuteru Kondo,[1] Yoshiyuki Ueno,[1] Koju Kobayashi,[2] Eiji Kakazu,[1] Masaaki Shiina,[1] Jun Inoue,[1] Keiichi Tamai,[1] Yuta Wakui,[1] Yasuhito Tanaka,[5] Masashi Ninomiya,[1] Noriyuki Obara,[1] Koji Fukushima,[1] Motoyasu Ishii,[3] Tomoo Kobayashi,[4] Hirofumi Niitsuma,[1] Satonori Kon,[2] and Tooru Shimosegawa[1]

[1]Division of Gastroenterology, Tohoku University Hospital, [2]School of Health Science, Tohoku University, [3]Department of Gastroenterology, Miyagi Social Insurance Hospital, and [4]Department of Gastroenterology, Tohoku Rosai Hospital, Sendai, and [5]Clinical Molecular Informative Medicine, Nagoya City University, Nagoya, Japan

Background. HBcAg-specific regulatory T (T_{reg}) cells play an important role in the pathogenesis of chronic hepatitis B. Soluble heat shock proteins, especially soluble heat shock protein 60 (sHSP60), could affect the function of T_{reg} cells via Toll-like receptor.

Methods. We analyzed the relationship between soluble heat shock protein production and hepatitis B virus (HBV) replication with both clinical samples from HBeAg-positive patients with chronic hepatitis B ($n = 24$) and HBeAb-positive patients with chronic hepatitis B ($n = 24$) and in vitro HBV-replicating hepatocytes. Thereafter, we examined the biological effects of sHSP60 with isolated T_{reg} cells.

Results. The serum levels of sHSP60 in patients with chronic hepatitis B were statistically significantly higher than those in patients with chronic hepatitis C ($P < .01$), and the levels of sHSP60 were correlated with the HBV DNA levels ($R = 0.532$; $P < .001$) but not with the alanine aminotransferase levels. Moreover, the levels of sHSP60 in HBV-replicating HepG2 cells were statistically significantly higher than those in control HepG2 cells. Preincubation of $CD4^+$ $CD25^+$ cells with recombinant HSP60 (1 ng/mL) statistically significantly increased the frequency of HBcAg-specific interleukin 10–secreting T_{reg} cells. The frequency of $IL7R^-CD4^+CD25^+$ cells, the expression of Toll-like receptor 2, and the suppressive function of T_{reg} cells had declined during entecavir treatment.

Conclusion. The function of HBcAg-specific T_{reg} cells was enhanced by sHSP60 produced from HBV-infected hepatocytes. Entecavir treatment suppressed the frequency and function of T_{reg} cells; this might contribute to the persistence of HBV infection.

Hepatitis B virus (HBV) is a noncytopathic DNA virus that causes chronic hepatitis and hepatocellular carcinoma as well as acute hepatitis and fulminant hepatitis [1]. HBV now affects more than 400 million people worldwide [2], and persistent infection develops in ~5% of adults and 95% of neonates who become infected with HBV.

It has been shown that the cellular immune system, including cytotoxic T lymphocytes, $CD4^+$ T helper 1 cells, and $CD4^+C25^+FoxP3^+$ regulatory T (T_{reg}) cells, plays a central role in the control of viral infection [3–6]. The hyporesponsiveness of HBV-specific T helper 1 cells and the excessive regulatory function of T_{reg} cells in peripheral blood in patients with chronic hepatitis B has been shown elsewhere [7–10]. Lamivudine treatment of chronic hepatitis B has been reported to restore both $CD4^+$ T cells and cytotoxic T lymphocyte hyporesponsiveness following the decrease of serum levels of HBV DNA and HBV-derived Ag [8, 11–13]. In our previous study, we observed that HBcAg-specific interleukin 10 (IL-10)–secreting T_{reg} cells could play an important role in the immunopathogenesis of chronic hepatitis B [9].

Received 14 July 2009; accepted 3 February 2010; electronically published 9 June 2010.

Potential conflicts of interest: none reported.

Financial support: Ministry of Health, Labor, and Welfare of Japan (Health and Labor Sciences Research Grants for the Research on Measures for Intractable Diseases); Ministry of Education, Culture, Sports, Science, and Technology of Japan (grant 21790642 to Y.K.).

Reprints or correspondence: Yoshiyuki Ueno, Division of Gastroenterology, Tohoku University Graduate School of Medicine, Seiryo 1-1, Aobaku, Sendai, 980-8574, Japan (yueno@mail.tains.tohoku.ac.jp).

The Journal of Infectious Diseases 2010;202(2):202–213

0022-1899/2010/20202-0004$15.00

DOI: 10.1086/653496

Table 1. Clinical Characteristics of Patients with Chronic Hepatitis B or Chronic Hepatitis C Included in This Study

Characteristic	Patients with chronic hepatitis B		Patients with chronic hepatitis C
	HBeAg-positive, HBeAb-negative patients	HBeAg-negative, HBeAb-positive patients	
Age, years	45.16 (12.46)	48.21 (10.23)	48.63 (7.96)
Sex, no. of patients			
Male	12	12	12
Female	12	12	12
ALT level, IU/L	76.91 (39.82)	75.96 (45.90)	76.21 (33.77)
HBV DNA level, log copies/mL	7.83 (0.86)	6.00 (0.81)	NA
Genotype, % of patients			
A	0	4.17	NA
B	12.5	8.33	NA
C	87.5	87.5	NA

NOTE. Data are mean values (standard deviations), unless otherwise indicated. ALT, alanine aminotransferase; HBV, hepatitis B virus; NA, not applicable.

Many research groups have reported the possible induction of anergy by T_{reg} cells, which constitutively express CD25 (the interleukin 2 receptor α chain) in the physiological state [14–16]. In humans, this population of T_{reg} cells, as defined by $CD4^+CD25^+CTLA4^+$ cells, $CD4^+CD25^+FoxP3^+$ cells, or $CD4^+CD25^+IL7R^-$ cells, constitutes 5%–10% of peripheral $CD4^+$ T cells and has a broad repertoire that recognizes various self and nonself antigens. It has been reported that T_{reg} cells have several different mechanisms in suppressing various kinds of immune cells [17, 18]. The important mechanisms are cell to cell contact and secretion of cytokines including IL-10 and transforming growth factor β (TGF-β) [19, 20]. HBcAg derived from HBV might induce T_{reg} cells to escape from immunological pressure, as reported in persistent infection with Epstein-Barr virus, hepatitis C virus (HCV), and human immunodeficiency virus type 1 [21–23]. Some results have indicated that reduction of HBV replication could reduce the frequency and/or function of T_{reg} cells in patients with chronic hepatitis B [4, 5, 8]. However, the key factors that affect HBcAg-specific T_{reg} cells in the replication of HBV remain unclear.

The mammalian 60-kDa heat shock protein is a many-faceted molecule. In addition to serving as a chaperone, heat shock protein 60 (HSP60) is expressed by different types of cells following their exposure to stress or immune responses and is present in the blood during inflammation [24–27]. Recently, HSP60 was reported to enhance the function of $CD4^+CD25^+$ regulatory T cell function via Toll-like receptor 2 (TLR2) signaling [28].

In this study, we investigated the serum level of HSP60 in patients with chronic hepatitis B and the relevance of HBcAg-specific IL-10-secreting T_{reg} cells and HSP60. We report evidence of the production of soluble HSP60 (sHSP60) from HBV-replicating hepatocytes, by use of clinical samples from patients with chronic hepatitis B and an in vitro HBV replication system. In addition, reductions of $CD4^+CD25^+IL7R^-$ T_{reg} cells and TLR2 expression on T_{reg} cells were observed during entecavir therapy. This study could contribute to better understanding of the immunopathogenesis of chronic hepatitis B and the development of immune-based treatment.

MATERIALS AND METHODS

Patients. Forty-eight patients with chronic hepatitis B were enrolled in this study (Table 1). The patients had serum levels of HBV DNA of >5.0 log copies/mL and had elevated alanine aminotransferase (ALT) levels (reference range, <40 IU/L) for >6 months prior to the study. To focus the analysis on the active phase of chronic hepatitis B, we excluded asymptomatic carriers and patients with immune tolerance by age (<30 years old), ALT values (<40 IU/L), and HBV DNA levels (<5.0 log copies/mL). Twenty-four patients were seropositive for HBeAg, and 24 patients were seropositive for anti-HBeAb. None of the patients tested positive for antibodies to hepatitis C virus or had liver disease due to other causes, such as alcohol, drugs, congestive heart failure, and autoimmune disease. Twenty-four patients with chronic hepatitis C and 10 healthy subjects were included as control subjects. Permission for the study was obtained from the Ethics Committee at Tohoku University Graduate School of Medicine (permission no. 2006-194]). Written informed consent was obtained from all the participants enrolled in this study. Participants were monitored for 6 months, and peripheral blood samples were obtained and assessed at 1, 2, 3, and 6 months. At each assessment, patients were evaluated for serum levels of HBV DNA, HBeAg, and anti-HBe, blood chemistry, and hematology. Levels of HBsAg, anti-HBs, total and immunoglobulin anti-HBc, HBeAg, anti-HBe, and anti-

hepatitis C virus were determined by means of commercial enzyme immunoassay kits (Abbott Laboratories). Serum levels of HBV DNA were measured by means of an Amplicor polymerase chain reaction (PCR) assay (lower limit of detection, 2.6 log copies/mL; Roche). High titers of HBV DNA were measured by means of a transcription-mediated amplification-hybridization protection assay (TMA; lower limit of detection, 3.7 log genome equivalents per milliliter). Data were adjusted by means of the following formula: Amplicor value = 0.83 × (TMA value) + 0.67.

Reagents. The following antibodies were used: CD3–allophycocyanin (APC), CD4–peridinin chlorophyll protein complex (PerCP), CD25–fluorescein isothiocyanate (FITC), CD25-phycoerythrin (PE), CD127-PE, Alexa Fluor 488 mouse anti–human CD282 (TLR2), CD284 (Toll-like receptor 4 [TLR4]), and isotype-matched control antibodies purchased from BD Bioscience. Recombinant HBcAg was obtained from Biodesign International. Recombinant HSP60 (rHSP60) was purchased from Stressgen.

Quantification of sHSP60 and soluble heat shock protein 70 (sHSP70) levels. Levels of HSP60 and heat shock protein 70 (HSP70) were quantified by use of HSP60 and HSP70 enzyme-linked immunosorbent assay (ELISA) kits (Stressgen). The serum samples from patients and supernatants from cell cultures were collected at sampling points and stocked at −20°C. The ELISA procedure was performed according to the manufacturer's protocol. First, 100-μL prepared samples were added to wells of anti-HSP60-coated plates. Then the reaction of the anti-HSP60 and horseradish peroxidase conjugate was performed after incubation and washing. Absorbance was measured at 450 nm. The HSP60 sample concentration was calculated by use of a standard curve.

Isolation of peripheral blood mononuclear cells (PBMCs) and T_{reg} cells. PBMCs were isolated from fresh heparinized blood by means of Ficoll-Hypaque density gradient centrifugation. T_{reg} cells were isolated by use of a Dynabeads regulatory $CD4^+CD25^+$ T cell kit (Invitrogen). T_{reg} cells were isolated according to the manufacturer's protocol. In brief, $CD4^+$ cells were isolated from PBMCs by means of negative selection. The remaining cells included the PBMCs depleted of $CD4^+$ cells. Then the $CD4^+CD25^+$ cells were selected positively by use of $CD25^+$ antibody combined with beads. Finally, the beads were detached by means of Detachabead (Invitrogen), because the function of T_{reg} cells might be modified by anti-CD25 antibody.

Coculture of γ-irradiated HBcAg-presenting antigen-presenting cells (APCs) and T_{reg} cells. During the isolation of T_{reg} cells, PBMCs depleted of $CD4^+$ cells could be obtained for use as APCs. PBMCs depleted of $CD4^+$ cells were stimulated at 1×10^6 cells/mL in Roswell Park Memorial Institute 1640 medium containing 10% fetal bovine serum with HBcAg (10 μg/mL) for 12 h at 37°C. Then these γ-irradiated cells were coincubated with 1×10^5 isolated T_{reg} cells that were untreated pretreated with TLR2 and TLR4 neutralizing antibody and rHSP60 (1 ng/mL) (Figures 1*A* and 2).

IL-10 secretion assay. Isolated T_{reg} cells were stimulated with HBcAg-presenting autologous γ-irradiated APCs for 12 h at 37°C. IL-10-secreting cells were stained by adding 10 μL of IL-10-detection antibody (PE-conjugated) together with anti-CD4-PerCP, anti-CD25-FITC, and anti-CD3-APC.

Flow cytometry. PBMCs were stained with CD3-APC, CD4-PerCP, CD25-FITC, and CD127-PE antibodies for 15 min on ice to analyze the frequency of $CD4^+CD25^+IL7R^-$ cells. CD4-PerCP, CD25-PE, and Alexa Fluor 488 mouse anti–human CD282 (TLR2) or CD284 (TLR4) were used for the analysis of TLR2 and TLR4 expression on $CD4^+CD25^+$ cells. Isotype-matched control antibodies were used for adjustment of the fluorescence intensity.

Construction of plasmids. The HBV plasmids was constructed as described elsewhere, with minor modifications [29]. In brief, a serum sample from one of the consecutive patients with fulminant hepatitis B (fulminant hepatitis clone 2), whose serum level of HBV DNA was the highest of the 5 patients, was used to extract total DNA (QIAamp DNA blood mini kit; Qiagen), which was subjected to nested PCR for 2 overlapping fragments; the amplified fragments were nucleotides 1051–3215/1–327 (2492 nucleotides; fragment A) and nucleotides 180–1953 (1774 nucleotides; fragment B). Then the vectors were digested with XbaI, and the XbaI-XbaI site of fragment A-pUC118 was ligated to the XbaI-XbaI site of fragment B-pUC118. Finally, a plasmid containing a 1.3-fold HBV genome (nucleotides 1051–3215/1–1953) was constructed and named pBFH2.

Cell culture and transfection. Human hepatoma HepG2 cells were incubated in Dulbecco modified Eagle medium supplemented with 10% bovine serum at 37°C and 5% carbon dioxide. For the assay of HBV replication, 6-well plates were seeded with 5×10^5 HepG2 or Huh7 cells each. On the next day, 1.5 μg of plasmid DNA were transfected to these cells by use of TransIT LT-1 transfection reagent (Mirus), and the culture supernatant and cells were collected 3 d later. The transfection efficiency was evaluated with a Great EscAPe secreted alkaline phosphatase reporter system 3 (Clontech), in which 10 ng/mL of a reporter plasmid expressing secreted alkaline phosphatase was cotransfected. Experiments were performed at least in triplicate.

Quantification of extracellular HBV DNA, HBsAg, and HBeAg levels. To digest the input plasmid DNA in the culture supernatant, 5 μL of the supernatant was treated with 5 U of DNase I (TaKaRa Bio) at 37°C for 1 h, and the reaction was stopped with edetic acid. Then total DNA was extracted with a QIAamp DNA blood mini kit, and 10 μL of 200-μL DNA solution was subjected to real-time PCR by use of a LightCycler

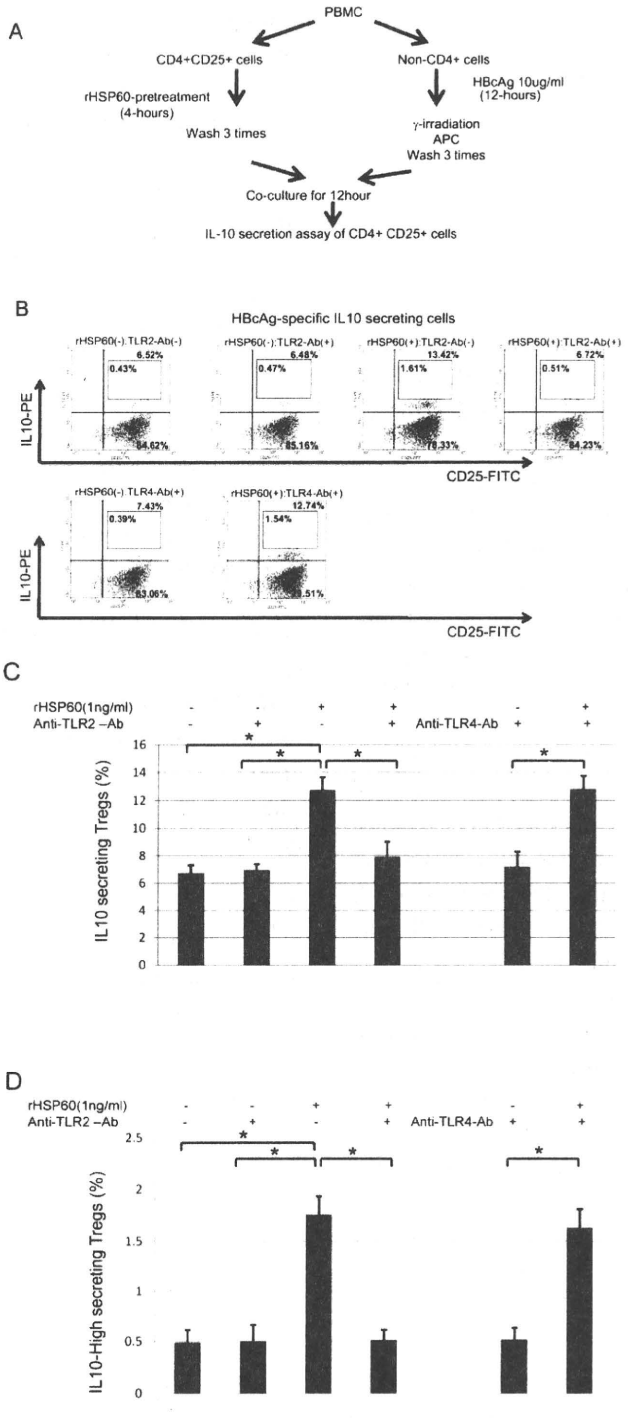

Figure 1. Effects of heat shock protein 60 (HSP60) on HBcAg-specific interleukin 10 (IL-10)–secreting regulatory T (T_{reg}) cells. *A,* Flow chart of the methods. *B,* Representative dot plots of IL-10-secreting cells in the $CD4^+CD25^+$ cells. The mixed cells (antigen-presenting cells [APCs; $CD4^-$] and isolated $CD4^+CD25^+$ cells) were stained with anti-CD4–peridinin chlorophyll protein complex (PerCP), anti-CD25–fluorescein isothiocyanate (FITC), and anti-IL-10-phycoerythrin (PE). The numbers in each top right quadrant indicate the frequencies of $CD25^+$ IL-10-secreting cells among the $CD4^+$ cells. The numbers in each bottom right quadrant indicate the frequencies of $CD4^+CD25^+IL\text{-}10^-$ cells among the $CD4^+$ cells. The numbers in each box in the top right quadrant indicate the frequencies of $CD25^+$ IL-10-secreting cells among the $CD4^+$ cells. *C,* Representative results for a sample from 1 patient with chronic hepatitis B (samples were obtained from 3 patients with chronic hepatitis B; this experiment was repeated 3 times). Bars indicate the percentage of IL-10-secreting cells among the $CD4^+$ cells with various kinds of pretreatment. *D,* Percentage of high–IL-10-secreting cells among the $CD4^+$ cells. Error bars indicate the standard deviation of 3 independent experiments with a sample from 1 patient with chronic hepatitis B. Three independent experiments yielded similar results to those shown in panels *C* and *D*. $^*P < .05$.

This figure is available in its entirety in the online version of the *Journal of Infectious Diseases*.

Figure 2. Effect of recombinant heat shock protein 60 (rHSP60) on the interleukin 10 (IL-10)–secreting activity of $CD4^+CD25^+$ cells.

system (Roche). ELISA kits were used to assay HBsAg (Hope Laboratories) and HBeAg (BioChain Institute) in 50 μL of the culture supernatant.

Sequence analysis of HBV DNA. The presence of HBV DNA in the serum samples was determined by means of PCR, as described elsewhere [30]. Nucleic acids were extracted from 100 mL of serum and subjected to nested PCR for the S gene. The amplification product of the first-round PCR was 461 bp, and that of the second-round PCR was 437 bp. The amplification products were sequenced directly on both strands by use of the BigDye Terminator Cycle Sequencing Ready reaction kit on an ABI Prism 3100 genetic analyzer (Applied Biosystems).

Carboxyfluorescein succinimidyl ester (CFSE) staining and suppression assay. The suppressive activity of regulatory T cells was analyzed by use of a CellTrace CFSE cell proliferation kit (Molecular Probes). Staining methods were followed according to the manufacturer's protocol. Briefly, the collected $CD4^+CD25^-$ cells were washed and resuspended in prewarmed phosphate-buffered saline with 0.1% bovine serum albumin at a final concentration of 3×10^5 cells/mL. CFSE solution (5 μm) was added and incubated at 37°C for 10 min. Stained cells were washed 3 times and incubated with unstained $CD4^+CD25^+$ T_{reg} cells and CD3CD28-coated stimulation beads (T cell expander) for an additional 3 d. The cells were analyzed by means flow cytometry with 488-nm excitation and emission filters.

Statistics. The data in Figures 3, 4, 1*C*, 1*D*, and 5 were analyzed by use of the independent *t* test. Statistical correlation analysis of the data in Figure 6 was performed by use of the Kendall τ_b test. The data in Figure 7 were analyzed by use of the Wilcoxon rank sum test. All of the statistical analyses were performed with SPSS software (version 10.0; SPSS). Results for which $P < .05$ were considered to be statistically significant.

RESULTS

Levels of sHSP60 and sHSP70 in samples from HBeAg-positive patients with chronic hepatitis B, HBeAg-negative patients with chronic hepatitis B, and control patients with chronic hepatitis C. The patients' characteristics, including age, sex, and ALT level, were matched among the different patient groups because the levels of sHSP60 and sHSP70 might be influenced by these factors (Table 1). The mean (± standard deviation [SD]) serum level of sHSP60 was 5.77 ± 1.19 ng/mL in HBeAg-positive patients with chronic hepatitis B, 4.12 ± 1.37 ng/mL in HBeAg-negative patients with chronic hepatitis B, 2.11 ± 0.96 ng/mL in patients with chronic hepatitis C, and 0.54 ± 0.46 ng/mL in healthy subjects. The levels of sHSP60 in patients with chronic hepatitis B (HBeAg-positive and HBeAg-negative) were statistically significantly higher than those in patients with chronic hepatitis C (Figure 3). On the other hand, the mean (± SD) serum level of sHSP70 was 7.89 ± 3.51 ng/mL in HBeAg-positive patients with chronic hepatitis B, 7.73 ± 3.71 ng/mL in HBeAg-negative patients with chronic hepatitis B, 8.09 ± 3.64 ng/mL in patients with chronic hepatitis C, and 3.54 ± 0.46 ng/mL in healthy subjects. There were no statistically significant differences in the level of sHSP70 between the chronic hepatitis B and chronic hepatitis C patient groups (Figure 3). Then we examined the correlations between the HSP60, HSP70, and HBV DNA or ALT levels. The levels of sHSP60 were correlated with the HBV DNA levels ($r = 0.532$; $P < .001$) but not with the ALT levels ($r = 0.101$; $P = .315$) (Figures 6*A* and 6*B*). On the other hand, the levels of sHSP70 were correlated with the ALT levels ($r = 0.520$; $P < .001$) but not with the HBV DNA levels ($r = 0.076$; $P < .449$) (Figure 6*C* and 6*D*).

HBV replication could directly induce sHSP60 production in vitro. Two kinds of plasmids carrying a 1.3-fold HBV genome that could replicate in HepG2 cells were used to analyze whether HBV replication could affect the production of sHSP60 in culture medium. The transfection efficiency was almost the

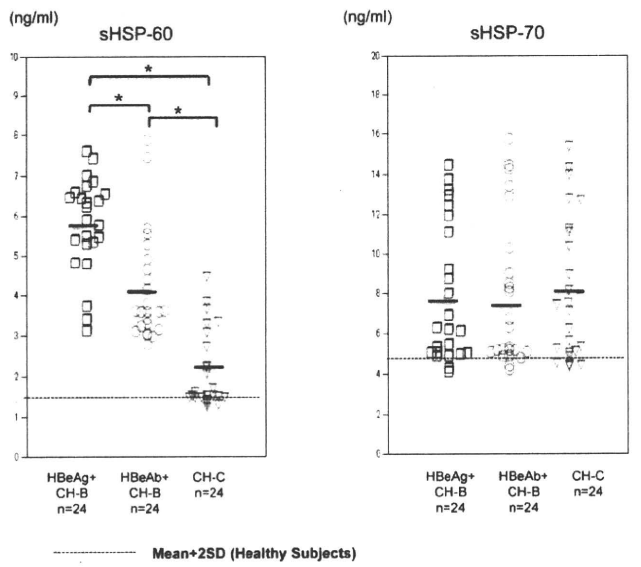

Figure 3. Quantification of serum levels of heat shock protein 60 (HSP60) and heat shock protein 70 (HSP70) in HBeAg-positive patients with chronic hepatitis B (CH-B), HBeAb-positive patients with CH-B, and patients with chronic hepatitis C (CH-C). Serum levels of HSP60 and HSP70 were quantified by means of enzyme-linked immunosorbent assay. The bar represents the means of the levels of HSP60 and HSP70. Dotted lines indicate the mean value plus 2 times the standard deviation (SD) of the levels of healthy subjects.

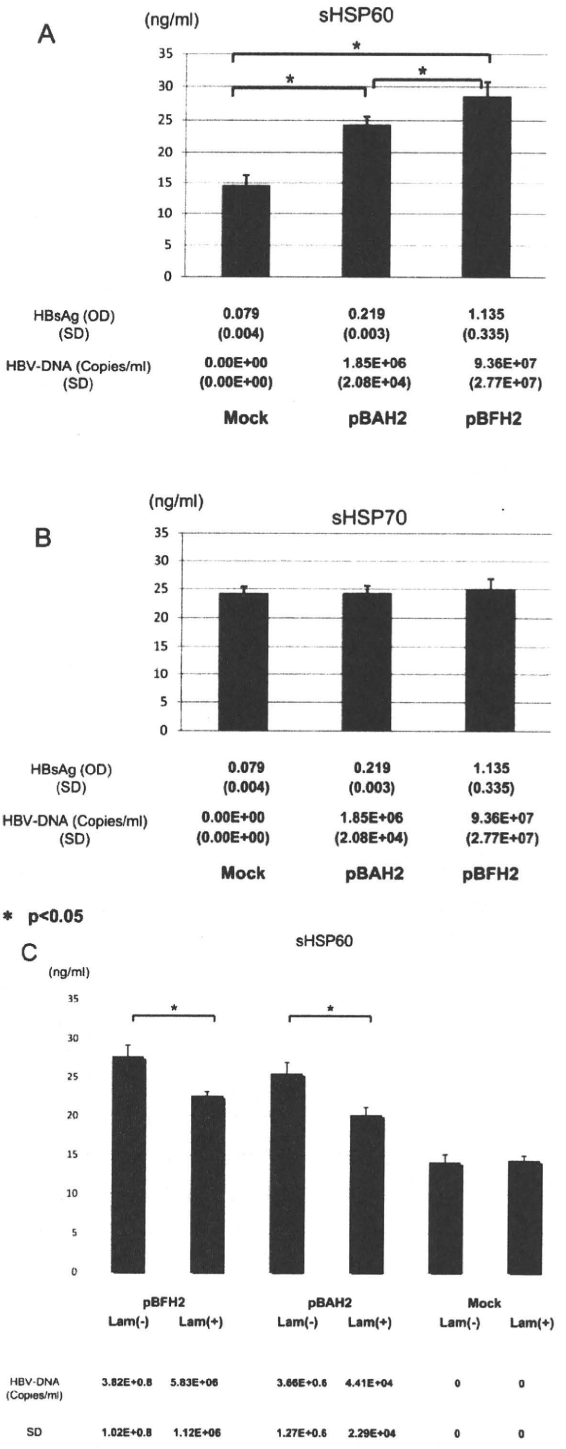

Figure 4. Direct effect of hepatitis B virus (HBV) on the production of heat shock protein 60 (HSP60) and heat shock protein 70 (HSP70). Two kinds of plasmid (pBAH2 and pBFH2) carrying a 1.3-fold HBV genome that could replicate in HepG2 cells and a mock plasmid were used to analyze whether HBV replication affects the production of soluble HSP60 (sHSP60) in culture medium. The levels of sHSP60 and soluble HSP70 (sHSP70) were compared among the 3 plasmid groups. Bars indicate the levels of HSP60 (*A*) and HSP70 (*B*). The HBsAg and HBV DNA levels and standard deviations (SDs) are included below the bar graphs. *C*, Levels of sHSP60 in cells with and those in cells without lamivudine treatment. The cells were treated with lamivudine (Lam; 0.5 μmol/L) for 72 h. Three independent experiments were performed.

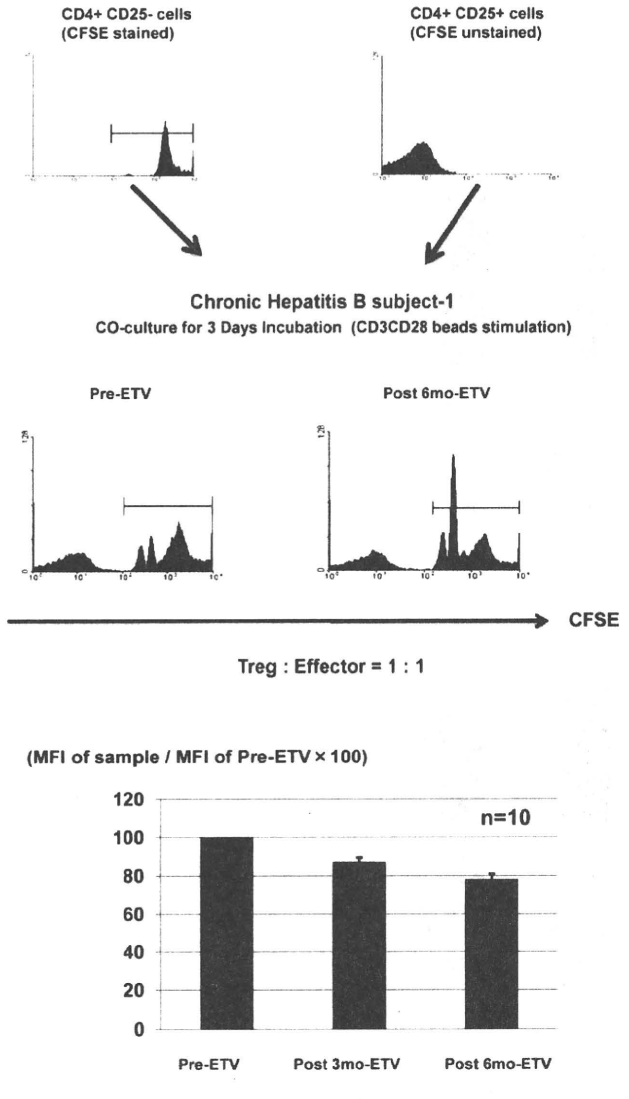

Figure 5. Suppression assay of regulatory T (T_{reg}) cells. The suppressive activity of T_{reg} cells was analyzed by means of coincubation of unstained isolated T_{reg} cells and autologous $CD4^+CD25^-$ cells with carboxyfluorescein succinimidyl ester (CFSE) staining. *A*, Representative histogram of CFSE-stained $CD4^+CD25^-$ effector cells and unstained $CD4^+CD25^+$ T_{reg} cells. *B*, Various levels of cell division in $CD4^+CD25^-$ effector cells observed 3 d after coincubation with CD3CD28-coated beads. *C*, Mean fluorescence intensity (MFI) of CFSE staining of $CD4^+CD25^-$ cells before treatment, 3 months after the start of entecavir (ETV) treatment, and 6 months after the start of entecavir treatment. The bars show the MFI of the samples divided by the MFI of the pretreatment samples ×100. The error bars indicate the standard deviations of the data.

same among the different plasmids (data not shown). The mean (± SD) HBV DNA levels of pBAH2 and pBFH2 were $1.85 \times 10^6 \pm 2.08 \times 10^4$ and $9.36 \times 10^7 \pm 2.77 \times 10^7$ copies/mL, respectively. The levels of sHSP60 in the supernatant of the pBAH2- and pBFH2-transfected HepG2 cells were statistically significantly higher than that of the mock-transfected HepG2 cells ($P < .05$) (Figure 4*A*). However, the levels of sHSP70 in the supernatant of the pBAH2- and pBFH2-transfected HepG2 cells were comparable with that of the mock-transfected HepG2 cells (Figure 4*B*). The addition of HBV-derived antigen in the culture supernatant could not increase the level of sHSP60 (data not shown). We performed the experiment on the suppression of HBV replication by nucleoside analogues in vitro. The suppression of HBV replication could statistically significantly reduce the production of sHSP60 (Figure 4*C*). These data indicate that HBV replication could increase the level of sHSP60 in the supernatant of the hepatocyte culture.

The effect of HSP60 on the HBcAg-specific IL-10-secreting T_{reg} cells. Previously, we found that HBcAg-specific IL-10-secreting cells could play an important role in the hyporesponsiveness of T cells in patients with chronic hepatitis B [9]. The effects of HSP60 on HBcAg-specific IL-10-secreting T_{reg} cells were analyzed. The appropriate dose of rHSP60 pretreatment was determined by use of PBMCs from healthy subjects (Figure 2). Pretreatment with rHSP60 could increase the frequency of HBcAg-specific IL-10-secreting cells statistically significantly ($P < .01$) and enhance the function of IL-10 secretion of HBcAg-specific T_{reg} cells, because the frequencies of high-intensity cells with IL-10 staining in HSP60 pretreatment T_{reg} cells were statistically significantly higher than those of control groups (Figure 1*D*). Moreover, these effects were completely blocked by neutralizing TLR2 antibody but not by TLR4 antibody. These data indicate that HSP60 might enhance the susceptibility and function of IL-10 secretion of HBcAg-specific T_{reg} cells.

Sequential analysis of clinical samples collected during entecavir therapy. Ten patients were selected for sequential analysis during entecavir therapy. The titers of HBV DNA and the ALT level rapidly decreased during entecavir therapy (Figures 7*A* and 7*B*). The serum levels of HSP60 had statistically significantly decreased at 3 months and at 6 months after the start of entecavir therapy. The frequency of T_{reg} cells and the expression level of TLR2 during entecavir treatment were quantified sequentially for up to 6 months during treatment by means of flow cytometry analysis. The frequency of $CD4^+CD25^+$ cells decreased, although not statistically significantly. On the other hand, the frequency of $CD4^+CD25^+IL7R^-$ cells (subpopulation of $CD4^+CD25^+$ cells) had statistically significantly decreased at 3 months and at 6 months after the start of entecavir therapy. The reason for the discrepancy could be that $CD4^+CD25^+$ cells included not only T_{reg} cells but also activated $CD4^+$ effector cells. Previously, some research groups had found that $CD4^+CD25^+FoxP3^+$ cells are almost the same as $CD4^+CD25^+IL7R^-$ cells. Therefore, our data indicate that entecavir therapy could reduce the frequency of T_{reg} cells. We also investigated the frequency of $CD4^+CD25^+FoxP3^+$ cells during lamivudine therapy (Figure 8). The frequency of